The Astrophysical Journal, 665:535–553, 2007 August 10

MEAN FIELD MAGNETOHYDRODYNAMICS OF ACCRETION DISKS

Frank H. Shu,[1] Daniele Galli,[2] Susana Lizano,[3] Alfred E. Glassgold,[4] and Patrick H. Diamond[1]

Received 2007 February 14; accepted 2007 May 2

ABSTRACT

We consider the accretion process in a disk with magnetic fields that are dragged in from the interstellar medium by gravitational collapse. Two diffusive processes are at work in the system: (1) "viscous" torques exerted by turbulent and magnetic stresses, and (2) "resistive" redistribution of mass with respect to the magnetic flux arising from the imperfect conduction of current. In steady state, self-consistency between the two rates of drift requires that a relationship exists between the coefficients of turbulent viscosity and turbulent resistivity. Ignoring any interactions with a stellar magnetosphere, we solve the steady-state equations for a magnetized disk under the gravitational attraction of a mass point and threaded by an amount of magnetic flux consistent with calculations of magnetized gravitational collapse in star formation. Our model mean field equations have an exact analytical solution that corresponds to magnetically diluted Keplerian rotation about the central mass point. The solution yields the strength of the magnetic field and the surface density as functions of radial position in the disk and their connection with the departure from pure Keplerian rotation in representative cases. We compare the predictions of the theory with the available observations concerning T Tauri stars, FU Orionis stars, and low- and high-mass protostars. Finally, we speculate on the physical causes for high and low states of the accretion disks that surround young stellar objects. One of the more important results of this study is the physical derivation of analytic expressions for the turbulent viscosity and turbulent resistivity.

Subject headings: accretion, accretion disks — MHD — planetary systems: protoplanetary disks — solar system: formation — stars: formation — turbulence

1. INTRODUCTION

It is universally acknowledged that magnetization is crucial to the accretion mechanism in circumstellar disks via the magneto-rotational instability (MRI) first studied in the nonlinear regime by Hawley & Balbus (1991; see Balbus & Hawley 1998 for a review). Since this accretion is the process by which most stars accumulate their masses from the gravitational infall of collapsing, rotating, molecular cloud cores (see, e.g., Shu et al. 1987; Evans 1999), and since planets are believed to form from the resulting circumstellar disks (e.g., Lissauer 1993; Papaloizou & Lin 1995; Lin & Papaloizou 1996; Goldreich et al. 2004), a better understanding of the mechanism of disk accretion (e.g., Lynden-Bell & Pringle 1974; Pringle 1981) is desirable for further progress in the fields of star and planet formation. Moreover, bipolar outflows and jets are ubiquitous in young stellar objects (YSOs; see Bachiller 1996; Reipurth & Bally 2001), while the best contemporary theories for the underlying collimated winds intimately involve the combination of rapidly rotating disks and strong magnetic fields, either threading the disk itself or belonging to the central host star (Königl & Pudritz 2000; Shu et al. 2000). A major uncertainty in the former models is the strength and geometry of the disk magnetic fields.

In this paper, we consider the global problem of the mass, angular-momentum, and magnetic-flux redistribution in disks around young stars that are threaded by interstellar fields dragged in by the process of gravitational collapse and infall. In a future extension of this work, we wish to include the interaction of such magnetized accretion disks at their inner edges with the stellar magnetosphere generated by dynamos operating in the central objects. Such interactions include the loss of angular momentum carried in any outflowing wind that develops at the surface of the parts of the disk that rotate sufficiently close to Keplerian rotation, a process that is examined in this paper only in terms of whether a wind's presence is implied by the prevailing circumstances. While separate pieces of this problem have been attacked by other groups (e.g., Goodson et al. 1999; Krasnopolsky & Königl 2002; Küker et al. 2004; Long et al. 2005), our study includes for the first time a perspective that combines analytical calculations with the likely levels of magnetic field brought into the disk of a YSO by gravitational collapse and infall (Galli et al. 2006; Shu et al. 2006).

Our paper builds on the prescient study of Lubow et al. (1994, hereafter LPP94) concerning the possibility of disk winds in accretion disks. What distinguishes our work from theirs is our concern with the much stronger magnetic fields resulting from the process of star formation than assumed by LPP94 (see § 3). Although LPP94 use a kinematic approximation that assumes explicitly an inward drift speed and implicitly a Keplerian rotation curve, neither assumption turns out to affect the generality of their solutions of the linear induction equation. Nevertheless, when fields are dynamically strong, a solution of the full magnetohydrodynamic (MHD) problem is required. Thus, an added component of our study is a physical formula for the viscosity associated with the MRI (see §§ 2.1 and 4.1). In other words, while LPP94 treat magnetic fields as a passive contaminant to an imposed accretion flow, we regard them as underlying the MRI dynamics that drives disk accretion. Our own theoretical work on the interaction of an electrically conducting accretion disk with a YSO magnetosphere that produces an X-wind and a funnel flow is incomplete because we previously ignored the magnetization of the accretion disk (see the review of Shu et al. 1999 and the criticisms of Ferreira et al. 2006).

[1] Department of Physics, University of California, San Diego, CA 92093; fshu@physics.ucsd.edu.
[2] INAF-Osservatorio Astrofisico di Arcetri, Largo E. Fermi 5, Firenze I-50125, Italy.
[3] CRyA, Universidad Nacional Autónoma de México, Apartado Postal 72-3, 58089 Morelia, Mexico.
[4] Astronomy Department, University of California, Berkeley, CA 94720.

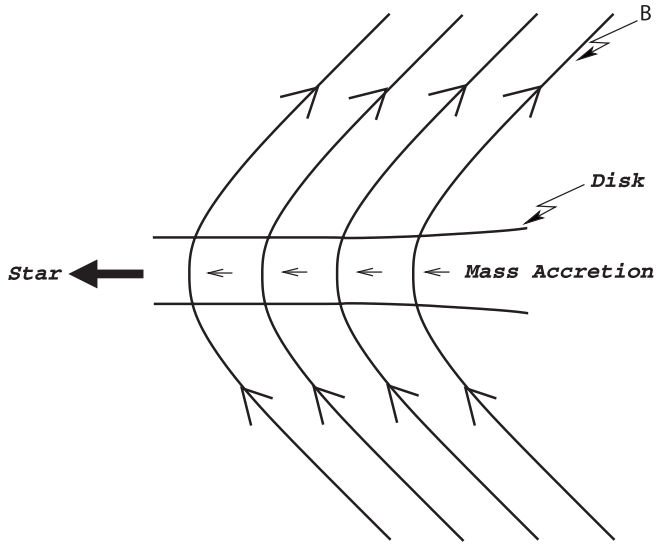

FIG. 1.—Schematic diagram of accretion flow in a disk threaded by magnetic flux accumulated by the process of star formation.

1.1. *Governing Equations*

We wish to calculate the effects of a systematically oriented, poloidal, mean magnetic field gathered from the interstellar medium that threads vertically through a circumstellar disk that surrounds a newly born star. This field is pinched radially inward by viscous accretion through the thin disk driven by the MRI (Fig. 1). To transform the usual 2.5D equations of nonideal MHD (with steep vertical stratification in z combined with full radial dependences in ϖ and axisymmetric motions in the tangential direction φ) to 1.5D (integration over z) requires that we explicitly treat the vacuum fields above and below the disk all the way out to infinity, which is a crucial missing ingredient in all numerical simulations of the MRI to date when global fields are present. Fortunately, this transformation can be implemented using the Green's function technique used by van Ballegooijen (1989) and LPP94 (see also Shu & Li [1997] and Shu et al. [2004], who were unaware of the earlier related work on accretion disks until the preparation of the present paper). In 1.5D, the formulation in terms of integrodifferential equations is then standard.

Terquem (2003; see also Fromang et al. 2005) made the interesting suggestion that toroidal magnetic fields in YSO disks might be strong enough to stop the so-called type I migration of planets and planetary embryos with Earth-like masses. The origin of such mean toroidal fields is unclear since they require unclosed z-currents and are subject to buoyant vertical loss through the Parker (1966) instability, but similar effects could arise for accretion-pinned poloidal distributions. The toroidal fields that arise in this paper from the stretching of radial fields by differential rotation vanish in the mean when we integrate over z. We shall treat their fluctuating effects on the turbulent transport of angular momentum and matter across field lines as diffusive terms in the nonideal equations of MHD with "anomalous" values for the coefficients of kinematic viscosity ν and electrical resistivity η (see §§ 2.1 and 4.1).

In such a mean field MHD treatment, the evolution of gas and magnetic field occurs in a thin, axisymmetric, viscously accreting disk surrounding a young star that we represent as a stationary and gravitating point of mass M_* at the origin of a cylindrical coordinate system $(\varpi,\ \varphi,\ z)$. We denote the disk's surface density by Σ, the radial velocity of accretion in the plane by u, the angular velocity of rotation about the z-axis by Ω, the component of the magnetic field threading vertically through the disk by B_z, and the radial component of the magnetic field just above the disk that responds to the radial accretion flow by B_ϖ^+. This self-gravitating, magnetized system satisfies the time-dependent equation of continuity,

$$\frac{\partial \Sigma}{\partial t} + \frac{1}{\varpi}\frac{\partial}{\partial \varpi}(\varpi \Sigma u) = 0, \tag{1}$$

the equation of radial-force balance,

$$-\varpi\Omega^2 = \frac{B_z B_\varpi^+}{2\pi\Sigma} - \frac{1}{\varpi^2}\left[GM_* + 2\pi\int_0^\infty K_0\left(\frac{r}{\varpi}\right) G\Sigma(r,\ t) r\, dr\right], \tag{2}$$

the torque equation, including phenomenologically the effect of turbulent viscous stresses ($\propto \nu$),

$$\Sigma\left(\frac{\partial}{\partial t} + u\frac{\partial}{\partial \varpi}\right)(\varpi^2\Omega) = \frac{1}{\varpi}\frac{\partial}{\partial \varpi}\left(\varpi^2 \Sigma \nu \varpi \frac{\partial \Omega}{\partial \varpi}\right), \tag{3}$$

and the induction equation for the vertical component of the magnetic field, including the effect of finite resistivity η,

$$\frac{\partial B_z}{\partial t} + \frac{1}{\varpi}\frac{\partial}{\partial \varpi}(\varpi B_z u) = -\frac{1}{\varpi}\frac{\partial}{\partial \varpi}\left(\frac{\varpi \eta}{z_0} B_\varpi^+\right), \tag{4}$$

where, according to Shu & Li (1997),

$$B_\varpi^+ = \int_0^\infty K_0\left(\frac{r}{\varpi}\right) B_z(r,\ t)\frac{r\, dr}{\varpi^2}. \tag{5}$$

In the vertical averaging over the thickness of the disk to arrive at equation (4), we have effectively replaced $\eta_{\rm local}\partial B_\varpi/\partial z$ by its mean value above the midplane of the disk, $\eta B_\varpi^+/z_0$, an operation that defines what we mean by average η. We shall later consider what we mean by the effective half-height of the disk, z_0 (see Appendix C), but for the time being we are content with the intuitive concept. Although it might be mathematically more elegant to absorb the combination η/z_0 into a single variable denoted, say, by a symbol $\mathcal{R}$, we retain the more cumbersome notation to keep better contact with the conventional microphysics of electrical resistivity. In any case, we assume that z_0 is much smaller than the local disk radius ϖ.

In equation (2), the first term on the right-hand side represents the mass per unit area, Σ, divided into the radial component of Lorentz force per unit area due to magnetic tension, $J_\varphi B_z/c$, where J_φ is the current density integrated over the thickness of the disk and equals $cB_\varpi^+/2\pi$ by Ampere's law. The second and third terms on the right-hand side represent the contributions to the force per unit mass associated with the stellar gravity of point mass M_* and the self-gravity of the gas of surface density Σ in the disk. To lowest order in the aspect ratio, $z_0/\varpi \ll 1$, we have neglected the pressure forces of the matter and the magnetic field (see Shu & Li 1997). The important astrophysical point is that the centripetal acceleration on the left-hand side of equation (2) is not given a priori but arises in response to the forces of (1) magnetic tension, (2) stellar gravity, (3) self-gravity of the disk gas, and (4) gas and magnetic pressure forces. We have ignored (4) explicitly, and we shall presently ignore (3) also. The rationale is that (3) and (4) are generally small in comparison with the stellar gravity term. Their inclusion would only yield small corrections at the expense of rendering the resulting problem intractable except by numerical attack. In contrast, the magnetic tension force is always present at

a level dictated by the amount (and distribution) of magnetic flux threading the disk.

The kernel in equation (5) is given by

$$K_0(\xi) \equiv \frac{1}{2\pi} \oint \frac{1 - \xi \cos\varphi}{(1 + \xi^2 - 2\xi \cos\varphi)^{3/2}} d\varphi. \tag{6}$$

The function $K_0(\xi)$ is plotted in Figure 1 of Shu et al. (2004) with mathematical properties described in their Appendix A. It has the asymptotic behaviors

$$K_0(0) = 1, \quad K_0(\xi) \to -\frac{1}{2\xi^3} \text{ as } \xi \to +\infty. \tag{7}$$

On a microscopic level, field diffusion in lightly ionized gases involves, in principle, three nonideal effects (see Wardle & Ng 1999): ohmic resistivity (because ions are knocked off field lines by collisions), the Hall effect (because electrons move differently than ions under electromagnetic fields and collisions), and ambipolar diffusion (because neutrals do not feel electromagnetic forces directly, but are subject to them indirectly because of collisions with the ions). For an axisymmetric problem, the Hall term vanishes, and the remaining two effects can be accorded the same treatment by defining an effective resistivity η given by the sum of the ohmic resistivity $\eta_{\rm ohm}$ and the contribution from ambipolar diffusion $\tau B_z^2/4\pi\rho$, where ρ is a representative local volume density and τ is the mean collision time for momentum exchange between a neutral particle and a sea of charged particles or particulates (if charged dust grains are important):

$$\eta = \eta_{\rm ohm} + \frac{\tau B_z^2}{4\pi\rho}. \tag{8}$$

For mean field magnetohydrodynamics, we assume that the same relation applies phenomenologically, and henceforth, when we speak of the "resistivity," we mean the effective value given by equation (8), appropriately generalized to include turbulent fluctuations. In Appendix A we comment on some alternative formulations of the turbulent diffusive processes that result in the same conclusions when the system is in steady state.

1.2. *Steady State*

In steady state with a spatially constant mass accretion rate $\dot{M}_d$, the equations of continuity, torque, and advection-diffusion of magnetic field simplify to

$$\varpi \Sigma u = \text{const} \equiv -\frac{\dot{M}_d}{2\pi}, \tag{9}$$

$$\dot{M}_d \varpi^2 \Omega = -2\pi\varpi^3 \Sigma \nu \frac{d\Omega}{d\varpi}, \tag{10}$$

$$B_z u = -B_z \frac{\dot{M}_d}{2\pi\varpi\Sigma} = -\frac{\eta B_\varpi^+}{z_0}, \tag{11}$$

whereas the centrifugal balance and the radial magnetic field B_ϖ^+ just above the disk plane are still given by equations (2) and (5) with no modifications except that there is no time dependence in the arguments of Σ and B_z. Elimination of $\dot{M}_d$ from equations (10) and (11) then yields the self-consistency requirement

$$\eta \frac{B_\varpi^+}{z_0 B_z} = -\frac{\nu}{\Omega} \frac{d\Omega}{d\varpi}. \tag{12}$$

In choosing the integration constants as above, we are implicitly allowing the origin (the star) to be a sink for mass but not for magnetic flux (or for angular momentum). To make this clearer, multiply equation (4) by $2\pi\varpi\, d\varpi$ and integrate in radius from the origin to a position just outside the star R_*^+ (which we will ultimately let $\to 0^+$). The result yields

$$\frac{d\Phi_*}{dt} = -2\pi R_* \left(B_z u + \frac{\eta B_\varpi^+}{z_0} \right)_{\varpi = R_*^+}, \tag{13}$$

where Φ_* is the magnetic flux accreted by the star. The assumption that equation (11) holds outside the star, in which the radial advection of magnetic field is everywhere balanced by the radial diffusion associated with diffusive effects, then implies that

$$\frac{d\Phi_*}{dt} = 0; \tag{14}$$

i.e., all the magnetic flux that is brought in by the gravitational collapse involved in star formation is contained in the disk, if the star plus disk forms a closed system. We emphasize that equation (14) is an *assumption*, not a deduction from first principles. It is astronomical observations, not theory, that tell us that little interstellar flux is brought inside stars. Indeed, Mestel & Spitzer (1956) already recognized more than 50 years ago that stellar fields would measure in the megagauss range if even a small fraction of the original interstellar flux were to appear on a young star's surface (see also Shu et al. 2004, 2006).

In this context, it is important to realize that magnetic reconnection will only destroy field lines that close within the disk. Indeed, the annihilation of field loops is essential for fluid transport through the disk, as discussed in § 4.1 below. In contrast, the open, mean magnetic fields pictured in Figure 1 have roots that extend to the interstellar medium. These field lines are responsible for the flux (integral of B_z over the area of the disk), and this flux cannot be lowered without modifying the interstellar currents (assumed to vanish at all finite distances in the derivation of eq. [5]), for example, by arbitrarily adding spatially large loops of current that yield a flux of opposite sign to the original interstellar value.[5]

In what follows, then, we choose to write equation (12) as

$$B_\varpi^+ = \alpha^2 B_z, \tag{15}$$

where we define the dimensionless auxiliary variable α by

$$\alpha^2 \equiv -\frac{z_0 \nu}{\varpi \eta} \left(\frac{\varpi}{\Omega} \frac{d\Omega}{d\varpi} \right). \tag{16}$$

For realistic configurations, we expect $B_\varpi^+ \sim B_z$; i.e., we anticipate that α is an order unity quantity. Since $\varpi\Omega^{-1} d\Omega/d\varpi$ is also

[5] One might still worry about the fate of open field lines with a fixed flux that connects a rapidly rotating disk with a slowly rotating interstellar cloud. Would not such field lines get twisted up in time and torque down the disk? The answer is yes, but for disturbances traveling a poloidal distance Δs along a field line out of the plane of the disk, the change in azimuthal angle $\Delta\varphi$ experienced by a loaded field line is approximately given by the disk rotation rate times the Alfvén crossing time across the region: $\Delta\varphi \sim \Omega(\Delta s/v_{\rm A})$. During the infall stage, the mass loading is so considerable that the ability even to form a disk is in jeopardy (see, e.g., Galli et al. 2006). After infall has stopped, the Alfvén speed $v_{\rm A}$ is very large near but above the disk, and it decreases as the field line begins to penetrate the interstellar cloud. In this stage, all the twist is at the cloud end; virtually none is at the disk end. In other words, eq. (25) below will hold to good approximation. There is little continued torquing of the disk because the rate of angular momentum transport per unit area by torsional Alfvén waves is limited by the angular momentum density $\rho\varpi^2\Omega$ times the Alfvén speed $v_{\rm A} = B/(4\pi\rho)^{1/2}$, with the small ρ above the disk of the former more than canceling the $\sqrt{\rho}$ in the denominator of the latter.

TABLE 1
Values of I_l and Inclination Angle i

Parameter	Values													
	$l = 0$	0.1	0.2	1/4	0.3	5/16	3/8	0.4	1/2	0.6	0.7	0.8	0.9	1
I_l	1	1.149	1.326	1.428	1.542	1.573	1.742	1.818	2.188	2.726	3.598	5.304	10.34	∞
i (deg)	45	49.0	53.0	55.0	57.0	57.5	60.1	61.2	65.4	69.9	74.5	79.3	84.5	90

of order unity, the resistivity η must be smaller than the (turbulent) viscosity ν by a factor given roughly by the local aspect ratio of the disk, i.e.,

$$\frac{\eta}{\nu} \sim \frac{z_0}{\varpi} \ll 1. \tag{17}$$

Equation (17) is in agreement with the assertion in equation (39) of LPP94 that the dimensionless ratio of interest is not η/ν but $(\eta/\nu)(\varpi/z_0)$, which must be of order unity for magnetic fields to be bent by an order unity amount from the vertical direction. The contrary assertion by Rüdiger & Shalybkov (2002) arises because they arbitrarily assume a uniformly rotating halo of conducting matter in which the differentially rotating disk is embedded. Some aspects of the problem that Rüdiger & Shalybkov consider could apply to the interaction of the inner edge of an accretion disk with a uniformly rotating stellar magnetosphere (e.g., Küker et al. 2004). The latter is the context of X-wind theory. In the next subsection, we give an explicit justification of the order-of-magnitude estimate in equation (17) when the disk mass is small enough to allow us to ignore its self-gravity.

1.3. *Exact Solution when Self-Gravity of the Disk Is Neglected*

If we may ignore the last term (disk self-gravity) in equation (2) in comparison to the other terms on the right-hand side (magnetic tension and stellar gravity), then the condition of centrifugal force balance becomes

$$\varpi\Omega^2 = -\frac{B_z B_\varpi^+}{2\pi\Sigma} + \frac{GM_*}{\varpi^2}, \tag{18}$$

where B_ϖ^+ is given by equation (5). Consider now the important case when Ω is appropriate for a thin disk in quasi-Keplerian rotation,

$$\Omega = f\left(\frac{GM_*}{\varpi^3}\right)^{1/2}, \tag{19}$$

where f is a constant less than 1 because of partial support of the disk against the stellar gravity by the magnetic tension of the poloidal magnetic fields that thread through it, brought into the system by the process of star formation. In order for these conditions to be mutually compatible, equation (18) requires

$$B_z = \alpha^{-1}\left[2\pi(1-f^2)GM_*\varpi^{-2}\Sigma\right]^{1/2}. \tag{20}$$

The substitution of equation (20) into equations (15) and (5) now results in a linear integral equation for $\Sigma^{1/2}$ when α is known,

$$\alpha(\varpi)\Sigma^{1/2}(\varpi) = \int_0^\infty K_0\left(\frac{r}{\varpi}\right)\alpha^{-1}(r)\Sigma^{1/2}(r)\frac{dr}{\varpi}. \tag{21}$$

Because $\Sigma^{1/2}$ enters linearly into equation (21) and α enters nonlinearly, the above relationship yields a constraint on the allowable solutions for both Σ and α. Consistent with equation (19), suppose, for example, that Σ is given by a power law:

$$\Sigma(\varpi) = C\varpi^{-2l}, \tag{22}$$

where C and l are constants. Then, equation (21) requires α^2 to be a positive dimensionless constant:

$$\alpha^2 = I_l \equiv \int_0^\infty K_0(\xi)\xi^{-l}\,d\xi. \tag{23}$$

The integral I_l has a finite value for l between -2 and 1 with $I_0 = 1$. Table 1 gives a tabulation of numerical values for the astronomically interesting range of l from 0 to 1 where Σ is a declining function of radius. The last row shows the inclination angle i that the surface field makes with respect to the vertical direction as computed from $\tan i = B_\varpi^+/B_z$ and equation (25) below.

Equations (23) and (19) now allow us to deduce from equation (16) the required relationship between the resistivity and viscosity as

$$\frac{\eta}{\nu} = \frac{3}{2I_l}\left(\frac{z_0}{\varpi}\right), \tag{24}$$

which supplies the missing numerical coefficient to our previous estimate (eq. [17]). The Prandtl combination η/ν is required in a steady-state accretion disk to have the specific ratio given by equation (24) if $u = -3\nu/2\varpi$ arising from the viscous transport of angular momentum (see eqs. [9] and [10]) is the same drift speed needed for the resistive diffusion of matter across stationary field lines, $u = -(\eta/z_0)B_\varpi^+/B_z$ (see eq. [11]). The two formulae for the drift velocity express succinctly why η only needs to be a small fraction of ν: unlike viscosity, resistivity is not acting to mix quantities on a large scale of ϖ; instead, it is trying to annihilate the oppositely directed mean radial fields B_ϖ on either side of the midplane distributed on a small scale z_0. If we consider the diffusivity associated with the *radial* distribution of the current J_φ (Appendix A), then that diffusivity η_J *is* approximately equal to ν.

The corresponding relationship between the radial component of the magnetic field at the upper surface of the disk and the vertical component at the midplane is given by equation (15) as

$$B_\varpi^+ = I_l B_z. \tag{25}$$

The vertical field is itself given by equation (20) when we know the surface density from equation (22), i.e.,

$$B_z = I_l^{-1/2}\left[2\pi(1-f^2)GM_*C\right]^{1/2}\varpi^{-(1+l)}. \tag{26}$$

To obtain the identification of the coefficient C, we note that equation (10) implies

$$\Sigma = \frac{\dot{M}_d}{3\pi\nu}. \tag{27}$$

Thus, the adoption of equation (22) is an implicit assumption that the viscosity varies as a power law of ϖ in steady state given by

$$\nu = \left(\frac{\dot{M}_d}{3\pi C}\right)\varpi^{2l}. \tag{28}$$

To make further progress, we need to have a physical theory for the kinematic viscosity ν (see §§ 2.1 and 4.1). This will allow the last unknown quantities l and C to be eliminated from our power-law solution for Ω, Σ, and B_z. We discuss first, however, in §§ 1.4 and 1.5 two results that hold for more general diffusivities.

1.4. *Disk Winds*

There are two criteria necessary for a cold wind to be magnetocentrifugally driven from the surface of a rotating disk (see the review of Königl & Pudritz 2000). Without detailed specifications of the physics of the viscosity or the resistivity, equation (25) allows us to confirm the conclusion reached by LPP94 concerning the first criterion:

$$\frac{B_\varpi^+}{B_z} = I_l \geq \frac{1}{\sqrt{3}}, \tag{29}$$

so that the footpoint field would then bend with an inclination angle i from the vertical by more than 30° (Chan & Henriksen 1980; Blandford & Payne 1982). Table 1 shows that the above criterion is comfortably satisfied for any disk where the surface density declines with radius, $l > 0$. In particular, $l = 1/4$ in equation (26) corresponds to the famous case $B_z \propto \varpi^{-5/4}$ considered by Blandford & Payne (1982) and yields $i = 55.0^\circ$. LPP94 state their wind-launching criterion in the form that $(\eta/\nu)(\varpi/z_0)$, which equals $3/(2I_l)$ according to equation (24), should be less than $1.52\sqrt{3}$. This result is almost identical to criterion (29). LPP94's calculation is for a finite disk with nonzero inner and outer radii, embedded in a background field of uniform strength pointing in the vertical direction, whereas our calculation is formally for an infinite disk with a trapped interstellar flux. The negligible astrophysical difference between 1.52 and 3/2 implies that none of these idealizations matter to the first criterion for driving a disk wind.

Unfortunately, the satisfaction of the magnetic criterion (29) by itself is not a sufficient condition for the appearance of a significant disk wind. Equation (48), derived from the consideration of vertical hydrostatic equilibrium, shows that if the fractional departure from Keplerian rotation $1 - f^2$ is large in comparison with the aspect ratio, $A \equiv z_0/\varpi$ divided by I_l, then the square of the characteristic thermal speed in the disk interior, a^2, is given by

$$a^2 \approx \frac{I_l}{2} A(1 - f^2)\frac{GM_*}{\varpi}. \tag{30}$$

On the other hand, in order to drive a disk wind, the square of the thermal speed at the disk surface, a_s^2, must be greater than a fraction (say, $\frac{1}{4}$) times the virial imbalance between the gravitational potential and twice the specific kinetic energy in disk rotation:

$$a_s^2 > \frac{1}{4}(1 - f^2)\frac{GM_*}{\varpi}. \tag{31}$$

The $\frac{1}{4}$ on the right-hand side has the following approximate justification. Parker's solution for a thermally driven spherical wind gives one factor of $\frac{1}{2}$ (see Parker 1963); this $\frac{1}{2}$ becomes $\frac{1}{4}$ because a particle in Keplerian rotation already has $\frac{1}{2}$ of the energy needed to escape. No other factors are then included because magnetocentrifugal effects do not help MHD winds in making the sonic transition (see the discussion of Shu et al. 1994).

Except for the effects of heating by external irradiation, the square of the thermal speed a_s^2 of the gas at the disk surface is likely to be small in comparison with its value a^2 in the disk interior when the disk is vigorously accreting, the condition needed to allow equation (48) to hold. Inequality (31) is then inconsistent with equation (30), implying that strong disk winds cannot be driven when $1 - f^2$ much exceeds the small number A (the disk aspect ratio z_0/ϖ). Otherwise, the surface that corresponds to smooth slow-MHD crossing would lie at so many scale heights above some nominal disk surface that the associated mass-loss rate would become negligibly small. LPP94 avoided this problem by their implicit assumption that the fields threading the disk were weak and therefore had no effect on the disk's assumed Keplerian rotation. Wardle & Königl (1993) examined the same issue in a *local* treatment of the launch region for disk winds assuming ambipolar diffusion to be the physical mechanism that loads field lines. They reported that the effect is present, but compensating factors exist that allow wind mass-loss rates to be a small fraction of the disk accretion rate, with a very sensitive dependence on the ratio of the orbit time to the ion-neutral collisional time τ (see Fig. 12 of their paper). The *global* treatment given in this paper, which includes an assessment of the likely levels of magnetic field strength to result from the process of star formation, indicates that the problem is more severe, perhaps even insurmountable for FU Orionis and T Tauri stars, although the situation may yet be rescued for the outer disk regions of embedded low- and high-mass protostars where A is not so small (see § 3).

Font et al. (2004) propose that photoevaporation is a more likely source of the slow, warm disk wind observed by Kwan et al. (2005) in T Tauri stars. A photoevaporative wind could reach a higher terminal velocity, but not a larger mass-loss rate (limited by the X-ray, EUV, or FUV photon flux reaching the surface of the disk at radii of a few AU or greater), because of the boost to the gas by magnetocentrifugal fling after the sonic transition is made. The combined effect could lead to a significant loss of angular momentum from the system in the late stages of YSO evolution that is not taken into account in our treatment. In other words, *outer* disk winds may realistically arise even if $1 - f^2$ is not small.

1.5. *Viscous and Resistive Dissipation Rates*

In steady state, the net emergent radiation from the upper and lower surfaces of a thin disk, after accounting for the irradiation of the central star, has to carry away the sum of the energies generated by viscous and resistive dissipation, whose rates per unit area are

$$\Psi = \nu\Sigma\left(\varpi\frac{d\Omega}{d\varpi}\right)^2 = \frac{3}{2}f^2\left(\frac{GM_*\dot{M}_*}{2\pi\varpi^3}\right), \tag{32}$$

$$Y \equiv J_\varphi E_\varphi = \left(\frac{cB_\varpi^+}{2\pi}\right)\left(-\frac{u}{c}B_z\right) = (1 - f^2)\frac{GM_*\dot{M}_d}{2\pi\varpi^3}. \tag{33}$$

In the above, $J_\varphi = cB_\varpi^+/2\pi$ and $E_\varphi = -uB_z/c$ are, respectively, the mean current density (integrated over z) and electric field in the φ-direction in the rest frame of the plasma tied to mean B_z relative to which the bulk of the matter in the disk is drifting at

radial velocity $u = -\dot{M}_d/2\pi\varpi\Sigma = -3\nu/2\varpi = -(\eta/z_0)B_\varpi^+/B_z$. To perform the last step in equation (33), we have used equations (18) and (19) to eliminate $B_\varpi^+ B_z/2\pi$ and Ω.

An alternative expression, $Y = \eta(B_\varpi^+)^2/2\pi z_0$, makes more apparent that Y represents the resistive dissipation, which feeds on the magnetic tension. In contrast, the viscous dissipation Ψ feeds on the disk shear. In the former case, a Lorentz force drives electric currents that generate heat by friction between the various charged and noncharged species; in the latter, heat is generated by fluid elements "rubbing" tangentially against each another. We speculate that a fraction of the energy released by resistive dissipation in the disk may go into accelerating suprathermal particles that give protoplanetary disks higher ionization rates than conventionally estimated (cf. Goldreich & Lynden-Bell 1969 vs. Sano et al. 2000).

The coefficient $3f^2/2$ in equation (32) differs from the standard result by the factor f^2 because the rotation law is only quasi-Keplerian, and implies a local rate of energy release 3 times as great as one might have expected from the loss of orbital energy because of accretion (see, e.g., Lynden-Bell & Pringle 1974). The difference is made up by a viscous torque that transfers energy from the inner disk to the outer disk, a debt that has to be repaid if we were to examine the details of the interaction of the disk near its inner edge with a star of finite size and, perhaps, magnetization. For example, if one applies a zero torque condition at an inner boundary R_x corresponding to a stellar magnetopause that corotates at the angular rate $\Omega(R_x) = f(GM_*/R_x^3)^{1/2}$, then standard arguments (Lynden-Bell & Pringle 1974) show that the total viscous energy dissipated by bringing matter through our accretion disk from infinity to R_x equals

$$\frac{1}{2}f^2\frac{GM_*\dot{M}_d}{R_x}. \tag{34}$$

In contrast, if we multiply equation (33) by $2\pi\varpi\, d\varpi$ and integrate from R_x to ∞, we derive that the rate of resistive dissipation of energy in the disk equals

$$(1-f^2)\frac{GM_*\dot{M}_d}{R_x}. \tag{35}$$

The sum of the viscous and resistive dissipation rates, equations (34) and (35), equals

$$\left(1-\frac{1}{2}f^2\right)\frac{GM_*\dot{M}_d}{R_x}, \tag{36}$$

which is not the total rate of gravitational potential energy release, $GM_*\dot{M}_d/R_x$, because an amount $R_x^2\Omega^2(R_x)/2 = f^2GM_*/2R_x$ is still retained by each gram of disk matter at the disk/stellar-magnetopause boundary as specific orbital energy. In actual practice, as will be shown in a future publication, f is raised to unity as the latter boundary is crossed by the swing of $B_\varpi^+ B_z$ from positive to negative values and inner-edge effects (assuming the magnetopause is not squashed by the accretion flow to the stellar surface in quasi–steady state), so $GM_*/2R_x$ of specific energy in the accreting matter is available for budgeting in a funnel flow or X-wind (Shu 1995). Note that in this description, electromagnetic fields, although responsible for the microphysics of viscous and resistive dissipation, act on the macroscale merely as catalysts for converting gravitational energy into other forms. These other forms, in steady state, involve no change of the magnetic energy because the magnetic fields have been assumed to remain constant in time.

Let us compare the expressions (32) and (33) that hold at radii $\varpi \gg R_x$. Then we easily calculate that heat generation by viscous dissipation dominates over resistive dissipation when $f > (2/5)^{1/2} = 0.6325$. The resistive contribution is typically not negligible; for example, it is 37.5% of the viscous contribution when $f = 0.8$. In spirit, if not in detail, our ideas then follow those of Lynden-Bell (1969), and we can imagine "resistive accretion disks" as well as their "viscous" counterparts (cf. the FU Orionis model of § 3).

2. VISCOSITY ASSOCIATED WITH MRI

Returning to our quest for the viscosity ν to be used in our power-law solution in § 1.3, we would like to benefit from the many numerical simulations that have been performed of the MRI since the pioneering studies of Balbus and Hawley. However, few experiments have been done that are of direct relevance to the problem in star formation that we address in this paper. Most simulations miss one or the other of the crucial ingredients of being both *global* and having *nonzero net flux*. When field lines extend to infinity (necessary to have nonzero net flux), rather than close within the system, consideration of the behavior of the field within a few vertical scale heights of a spatially thin disk suffices only if one has included knowledge of what those fields do at large distances. The application of boundary conditions at smaller distances will generally exert extraneous stresses. Because of these difficulties, many simulations are both local and have zero net flux, in that a small portion of a shearing sheet or layer is threaded by mean vertical magnetic fields B_z inputted initially to vary sinusoidally in the radial direction. Radial mixing and reconnection can destroy most of the initial vertical field in such simulations, so that the turbulent state reached asymptotically in time is largely independent of the assumptions of the "initial" state. The finely resolved study by Silver & Balbus (2006) does include the effect of a systematically directed field B_z of a single sign, but their simulation is not global (and therefore does not develop a B_ϖ^+ comparable to B_z), and it is performed for a gas pressure 800 times larger than the magnetic pressure, i.e., with implied magnetic fields that are too weak to be useful for our studies here.

Stone et al. (1996) and Miller & Stone (2000) performed, to our knowledge, the only well-known simulations of a thin disk threaded by a systematic, large-scale, nonzero, vertical field B_z. The computations were semiglobal in spanning a larger than usual, but still limited, range of z. (The work by Fleming et al. [2000] assumes periodicity in the z-direction, which does not faithfully represent the dynamics of a thin disk.) The thin-disk cases with nonzero net flux behave completely differently from the other more frequently studied configurations, whose initial states have only toroidal fields, or, at least, zero average B_z. The systems in the simulations of Stone et al. (1996) and Miller & Stone (2000) quickly become magnetically dominated, unlike the usually considered circumstance where the gas pressure is much greater than the magnetic pressure. The rapid evolution then prevented the authors from examining the astrophysical consequences of the configuration most likely to be relevant to investigations in star formation.

2.1. *Turbulent Viscosity*

In the absence of relevant numerical simulations, we give the following order-of-magnitude argument on the basis of mixing-length ideas (Prandtl 1925). When a radial field B_ϖ is present in a field of differential rotation, we expect that field to be sheared and yield an azimuthal component B_φ. The tendency for electrically conducting fluids to flow along the field direction suggests

that fluctuations in the radial velocity δu will be related to the horizontal fields and the shear rate by

$$B_\varphi \delta u \sim B_\varpi \varpi \frac{d\Omega}{d\varpi} \delta\varpi, \tag{37}$$

where $\delta\varpi$ is the radial mixing length and has the same sign as δu. Note that the induced B_φ has systematically the opposite sign as B_ϖ if $d\Omega/d\varpi$ is negative. The systematics of B_φ relative to B_ϖ lead to the desired "viscous" torque.

Differentially rotating fluid parcels displaced from their equilibrium positions that preserve their specific angular momentum gyrate in epicycles about a guiding center characterized by an epicyclic frequency κ that numerically equals Ω in a quasi-Keplerian disk (Binney & Tremaine 1987, p. 120). Although other forces are also at play in a magnetized accretion disk, we assume that mixing-length scales of greatest interest for the transport of angular momentum have a correlation time between $\delta\varpi$ and δu that is similarly given by $\sim\Omega^{-1}$, i.e.,

$$\delta u \sim \Omega \delta\varpi. \tag{38}$$

Equation (37) can now be written

$$B_\varphi \sim B_\varpi \frac{\varpi}{\Omega} \frac{d\Omega}{d\varpi}. \tag{39}$$

The component of Maxwell stress responsible for exerting torque, $B_\varpi B_\varphi/4\pi$, integrated over the thickness of the disk, can then be approximated as

$$\mathcal{F} \frac{(B_\varpi^+)^2}{2\pi} \frac{\varpi}{\Omega} \frac{d\Omega}{d\varpi} z_0, \tag{40}$$

where $\mathcal{F}$ is a form factor that comes from the vertical integration, and that also corrects for all the order-of-magnitude approximations used to arrive at this point. If the term (40) is the dominant contribution to the "viscous" stress modeled in equation (3), then the associated "kinematic viscosity" equals

$$\nu = \mathcal{F} \frac{(B_\varpi^+)^2 z_0}{2\pi\Sigma\Omega}. \tag{41}$$

A more picturesque "derivation" of equation (41) that explains why the correlations do not involve quadratic products of fluctuating quantities (they actually do) and why the mixing length $\delta\varpi$ seemingly dropped out of the calculation (it should not) is given in § 4.1. We proceed here to build confidence in the case by first demonstrating that the adoption of equation (41) leads to reasonable astrophysical results.

To follow the flux redistribution, our problem is formulated using B_z rather than B_ϖ^+, so in steady state we set $B_\varpi^+ = I_l B_z$ (cf. eq. [25]) and get

$$\nu = D \frac{B_z^2 z_0}{2\pi\Sigma\Omega}, \tag{42}$$

where D is a dimensionless coefficient given by $D = I_l^2 \mathcal{F}$. Although $\mathcal{F}$ is the more fundamental quantity, as we shall see in a later study of the interaction of disks with stellar magnetospheres, we shall use D in this paper as the relevant dimensionless parameter to obtain ν from observations and simulations (see the discussion of Appendix B). As long as $\mathcal{F}$ is not too small compared to unity, D is an order unity quantity, provided the entire disk layer undergoes vigorous mixing from the MRI.

With ν given by equation (42), equation (27) yields the following expression for the vertical magnetic field:

$$B_z = \left(\frac{2f}{3DA}\right)^{1/2} \left(\frac{GM_* \dot{M}_d^2}{\varpi^5}\right)^{1/4}, \tag{43}$$

where we have used equation (19) to express the angular rotation rate Ω and where $A \equiv z_0/\varpi$ is the aspect ratio of the local disk height to disk radius. From equations (20) and (48), we are then able to recover the surface density as

$$\Sigma = \frac{f}{1-f^2} \left(\frac{I_l}{3\pi DA}\right) \frac{\dot{M}_d}{(GM_*\varpi)^{1/2}}. \tag{44}$$

Equation (42) holds with nonzero D only as long as (1) good magnetic coupling exists, and (2) the criterion for the MRI instability is satisfied, that the magnetic pressure be smaller than the gas pressure. If we define a fiducial square of the thermal velocity $a^2(\varpi)$ by the gas pressure at the midplane, $P(\varpi, 0)$, divided by the characteristic volume-density in the disk, $\Sigma(\varpi)/2z_0(\varpi)$, equations (43) and (44) imply that the ratio of the magnetic pressure to gas pressure at the disk's midplane is then given by

$$\frac{B_z^2 z_0}{4\pi\Sigma a^2} = \frac{(1-f^2)}{2I_l} \left(\frac{AGM_*}{a^2\varpi}\right), \tag{45}$$

where we have expressed $z_0 = A\varpi$. On the other hand, analysis of the vertical hydrostatic equilibrium of the disk using the method of Wardle & Königl (1993; see also Ogilvie 1997; Shu & Li 1997) gives (see Appendix C):

$$a^2 = \frac{1}{2}\left[I_l(1-f^2)A + A^2\right] \frac{GM_*}{\varpi}. \tag{46}$$

In principle, a proper physical treatment would require us to obtain $a^2(\varpi)$ by computing the volumetric viscous and resistive heating as a function of z and balance it against the heat transported by radiative transfer and thermal convection vertically out of the disk. Once we have obtained $a^2(\varpi)$, we could then solve equation (46) as a quadratic equation for the disk aspect ratio A. Such a physically involved treatment is beyond the scope of the present paper, and for the astronomical and pedagogical sake of obtaining numerical examples, we shall assume the luxury of specifying $A(\varpi)$ semiempirically as a power law (see § 2.3).

The justification for approximating A as a power law follows. If disks are spatially thin, A is small compared to unity. There are then two different regimes of physical interest. The first case arises when the departure $(1-f^2)$ from Keplerian rotation is small and the first-term on the right-hand side of equation (46) is negligible in comparison with the second term, resulting in the approximation

$$A \approx a\sqrt{\frac{2\varpi}{GM_*}} \quad \text{for} \quad 1-f^2 \ll \frac{A}{I_l}. \tag{47}$$

In case (47), the contribution of the magnetic pressure is ignorable for the vertical hydrostatic equilibrium, and the draw of the stellar gravity toward the midplane keeps a cool accretion disk spatially thin. The second case arises when the departure from Keplerian rotation $(1-f^2)$ is not small and the first-term on the right-hand side of equation (46) dominates over the second:

$$A \approx \frac{2}{I_l}\left[\frac{a^2\varpi}{GM_*(1-f^2)}\right] \quad \text{for} \quad 1-f^2 \gg \frac{A}{I_l}. \tag{48}$$

In case (48), the disk is kept spatially thin, not by stellar gravity but by the inward press of the component of magnetic pressure $B_\varpi^2/8\pi$, which increases outward from the midplane $z = 0$, where its value is 0, to the surface, where its value is $(B_\varpi^+)^2/8\pi = I_l^2 B_z^2/8\pi$.

From the community experience in disk thermal physics, it is well known that numerical solutions frequently show two types of power-law solutions for the vertically averaged temperature $\propto a^2(\varpi)$, namely, $a^2 \propto \varpi^{-3/4}$ for passive, irradiated disks, and $a^2 \propto \varpi^{-1/2}$ for active, accretion-powered disks. For $a^2 \propto \varpi^{-3/4}$, case (47) yields $A(\varpi) \propto \varpi^{1/8}$ and case (48) yields $A(\varpi) \propto \varpi^{1/4}$. For $a^2 \propto \varpi^{-1/2}$, case (47) yields $A(\varpi) \propto \varpi^{1/4}$ and case (48) yields $A(\varpi) \propto \varpi^{1/2}$. Therefore, a power-law description for disk flaring, $A(\varpi) \propto \varpi^n$, with $n = 1/4$ typically or $n = 1/8$ or 1/2 at the extremes, has a theoretical basis.

Apart from the issue of sufficient ionization, the requirement for MRI being present in the midplane is that the left-hand side of equation (45) should be less than unity. This requirement is *automatically* satisfied for all our disks because the substitution of equation (46) into the right-hand side of equation (45) gives a value $(1 - f^2)/[(1 - f^2)I_l^2 + AI_l]$, which is always smaller than 1 for $I_l \geq 1$, i.e., for $l \geq 0$ (Table 1). In particular, in the regime where equation (48) holds, ν from equation (42) becomes

$$\nu = \frac{2D}{I_l^2}\left(\frac{a^2}{\Omega}\right), \tag{49}$$

which has the same form as the Shakura & Sunyaev (1973) viscosity, $\nu \equiv \alpha_{\rm ss} a^2/\Omega$ with $\alpha_{\rm ss} = 2D/I_l^2$. The strongly magnetized disks of this paper therefore both automatically satisfy the criterion that MRI exist in the midplane and have equivalent Shakura-Sunyaev α-values of order unity if $D \sim 1$. By compressing the midplane gas density and pressure to higher values than gravity can achieve alone, such disks always operate at nearly the maximum efficiency for viscous transport, if $D \sim 1$, without shutting down the MRI. Aficionados of MRI like to say that it is present in thin disks for arbitrarily low levels of magnetic field; now they can add that it is present for arbitrarily high values too, provided $I_l = B_\varpi^+/B_z \geq 1$.

For later reference in discussions of disk fragmentation, we record that the local dimensionless mass-to-flux ratio in the disk is given by (see Nakano & Nakamura 1978; Basu & Mouschovias 1994; Shu & Li 1997; Krasnopolsky & Gammie 2005)

$$\lambda \equiv \frac{2\pi G^{1/2}\Sigma}{B_z} = \frac{I_l}{1 - f^2}\left(\frac{2f}{3DA}\right)^{1/2}\left(\frac{\dot{M}_d^2 \varpi^3}{GM_*^3}\right)^{1/4}. \tag{50}$$

The supercritical condition $\lambda > 1$ is necessary, but not sufficient, for local disk fragmentation. We must also examine, at least, the Toomre (1964) Q parameter, which for gaseous disks must be less than unity for local gravitational instability. Thus, also for later reference, we note that associated with equation (46) is a Toomre Q, which is given by the formula $Q = \Omega a/\pi G\Sigma$ for a disk in quasi-Keplerian rotation. In principle, a should be computed from the considerations of heat balance outlined earlier, but for fiducial purposes, we use the value of a associated with case (48):

$$Q = \frac{3}{\sqrt{2I_l}} D\left[A(1 - f^2)\right]^{3/2}\left[\frac{M_*}{\dot{M}_d}\left(\frac{GM_*}{\varpi^3}\right)^{1/2}\right]. \tag{51}$$

In what follows, we take the combination $\lambda > 1$ and $Q < 1$ as necessary indicators of local gravitational instability. With a "standard" flaring law, $A \propto \varpi^{1/4}$, both criteria favor the outer regions of a disk for the possible occurrence of disk fragmentation.

Finally, for arbitrary values of f, equations (27) and (24) give the viscosity and resistivity generated by the MRI instability in the disk as

$$\nu = \frac{AD(1 - f^2)}{fI_l}(GM_*\varpi)^{1/2}, \tag{52}$$

$$\eta = \frac{3A^2 D(1 - f^2)}{2fI_l^2}(GM_*\varpi)^{1/2}. \tag{53}$$

Apart from the factors involving A, D, and f, these expressions show that the natural scaling for both diffusivities is the specific angular momentum of the matter in Kepler orbits, $(GM_*\varpi)^{1/2}$. Note especially the lack of any parametric dependence on the assumed mass accretion rate $\dot{M}_d$.

2.2. *Enclosed Disk Mass, Magnetic Flux, and Angular Momentum*

To make equations (43) and (44) consistent with equations (26) and (22), the product DA has to be a power law of ϖ. We adopt the natural assumptions that D equals a constant and the disk flares as a power law, so that the aspect ratio $A(r)$ at radius r is related to its value $A(\varpi)$ at radius ϖ by the formula

$$A(r) = A(\varpi)(r/\varpi)^n, \tag{54}$$

where n is the flaring exponent, which is positive definite if shadowing does not occur. Had we adopted these assumptions from the start, together with the hypothesis (42), we could have shown that not only are the discovered power-law solutions possible in steady state, but they are unique. The relationship between the exponent n and the exponent l in equation (22) can be found from equation (44) with $A(\varpi) \propto \varpi^n$, namely, $-2l = -n - 1/2$, or

$$l = (1 + 2n)/4. \tag{55}$$

For later reference we note from Table 1 that $I_l = 1.573$, 1.742, or 2.188 for disks with low, typical, or high power-law flaring, $n = 1/8$ and $l = 5/16$ (i.e., $\Sigma \propto \varpi^{-5/8}$), $n = 1/4$ and $l = 3/8$ (i.e., $\Sigma \propto \varpi^{-3/4}$), or $n = 1/2$ and $l = 1/2$ (i.e., $\Sigma \propto \varpi^{-1}$), respectively.

We wish now to compute the enclosed mass in the disk inside a radius ϖ,

$$M_d(\varpi) \equiv 2\pi \int_0^\varpi \Sigma(r) r\, dr = \left[\frac{4I_l}{3(3 - 2n)}\right]\left(\frac{f}{1 - f^2}\right)\left[\frac{1}{DA(\varpi)}\right]\frac{\dot{M}_d}{(GM_*/\varpi^3)^{1/2}}. \tag{56}$$

Thus, $M_d(\varpi)$ is a multiple of the mass that accretes through the disk during a Keplerian rotation period at that radius. This multiple depends on the combination $(DA)^{-1}$ and on the effective value of f. Except for a numerical factor of order unity, we easily verify the interpretation that the enclosed mass $M_d(\varpi)$ results from accretion at a rate $\dot{M}_d$ over a viscous diffusion timescale ϖ^2/ν.

According to the discussion in § 1.2, the magnetic field brought in by infall is contained as magnetic flux threading the disk.

Inside any radius ϖ where the disk is in steady state the enclosed magnetic flux is given by

$$\Phi_d(\varpi) \equiv 2\pi \int_0^{\varpi} B_z(r) r\, dr = 2\pi \left(\frac{4}{3-2n}\right) \left[\frac{2f}{3DA(\varpi)}\right]^{1/2} \left(GM_* \dot{M}_d^2 \varpi^3\right)^{1/4}. \quad (57)$$

If the disk's mass is negligible in comparison with the star's, the system's dimensionless mass-to-flux ratio enclosed inside ϖ equals

$$\lambda_*(\varpi) \equiv \frac{2\pi G^{1/2} M_*}{\Phi_d(\varpi)} = \left(\frac{3-2n}{4}\right) \left[\frac{3DA(\varpi)}{2f}\right]^{1/2} \left(\frac{GM_*^3}{\dot{M}_d^2 \varpi^3}\right)^{1/4}. \quad (58)$$

Infall models with field freezing until small radii yield $\lambda_* \approx 1$–4 (Galli et al. 2006), consistent with the polarization findings of Girart et al. (2006) of an hourglass shape in NGC 1333 IRAS 4A. Field slippage during the collapse reduces the enclosed flux for a low-mass protostar by a further factor of 2–3 at the radii $\sim$300 AU that their disks are likely to occupy (see Fig. 3 of Shu et al. [2006] when $R_{\rm ohm}$ in that paper has a value $\sim$10 AU). Thus, in § 3 we adopt an enclosed mass-to-flux value of $\lambda_0 = 4$ for the system as a typical outcome of the star and disk formation process. If insufficient time has elapsed for the disk to reach steady state inside the radius where $\lambda_* = \lambda_0$, investigations of the affected regions should make use of the time-dependent equations with which we began this paper (§ 1.1).

It is extremely informative to compute the enclosed mass at a radius R_Φ where $\lambda_*(R_\Phi) = \lambda_0$, i.e., at a radius where the disk contains the entire flux brought in by star formation:

$$M_d(R_\Phi) = \left[\frac{(3-2n) I_l}{8\lambda_0^2}\right] \frac{M_*}{1-f^2}. \quad (59)$$

For the typical case, $n = 1/4$, $l = 3/8$, and $I_l = 1.742$, equation (59) becomes

$$1 - f^2 = \left(\frac{0.5444}{\lambda_0^2}\right) \frac{M_*}{M_d(R_\Phi)}. \quad (60)$$

For a closed system in which infall has ceased, so that λ_0 remains a fixed constant, disk accretion must decrease $M_d(R_\Phi)$ relative to M_*, and therefore the departure from Keplerian rotation, $(1 - f^2)$, must grow with time. This trend arises because viscosity drains mass from the disk onto the star, while resistivity can only cause the redistribution of flux within the disk but cannot change the total, making the specific magnetization (inverse λ) rise with time. In § 3 we combine equation (60) with an assumption of a disk's "age" to estimate the numerical value of the important parameter f.

To appreciate concisely the dynamical consequences of disk magnetization, we note that equations (50) and (58) imply the interesting reciprocity relationship

$$\lambda(\varpi)\lambda_*(\varpi) = \left(\frac{3-2n}{4}\right)\left(\frac{I_l}{1-f^2}\right), \quad (61)$$

where the right-hand side is a constant that depends only on f and $l = (1 + 2n)/4$. Except for such constants, a similar relationship was derived by Shu et al. (2004) in their analysis of magnetic levitation of pseudodisks by strongly magnetized central objects (see their eq. [65]). Although disks differ from pseudodisks in being (partially) centrifugally supported, and although the inner parts of a magnetized disk differ from a split monopole in their detailed interaction with the outer parts of the same magnetized disk, the principles are qualitatively similar and provide physical insight into why such magnetic support (levitation of the outside by the inside) causes the rotation to occur at sub-Keplerian rates.

Finally, if the mass is mostly in M_*, the enclosed angular momentum of the parts of the disk that are in steady-state accretion is given by

$$\mathcal{J}_d = 2\pi \int_0^{\varpi} \Sigma(r) r^2 \Omega(r) r\, dr = f\left(\frac{3-2n}{4-2n}\right) M_d(\varpi)(GM_*\varpi)^{1/2}. \quad (62)$$

Equations (57), (56), and (62) show that the enclosed disk flux, mass, and angular momentum represent a sequence of decreasing central concentration.

2.3. *Seminumerical Formulae*

For the convenience of the reader, we express the results of the analytical theory in the following seminumerical form:

$$B_z(\varpi) = 8.89 \times 10^{-3} D^{-1/2} \left(\frac{M_*}{0.5\ M_\odot}\right)^{1/4} \times \left(\frac{\dot{M}_d}{2\times 10^{-6}\ M_\odot\ {\rm yr}^{-1}}\right)^{1/2} \times f^{1/2} \left[\frac{0.1}{A(\varpi)}\right]^{1/2} \left(\frac{\varpi}{100\ {\rm AU}}\right)^{-5/4} {\rm G}, \quad (63)$$

$$\Sigma(\varpi) = 0.740 D^{-1} \left(\frac{M_*}{0.5\ M_\odot}\right)^{-1/2} \left(\frac{\dot{M}_d}{2\times 10^{-6}\ M_\odot\ {\rm yr}^{-1}}\right) \times \left(\frac{f}{1-f^2}\right) \left[\frac{0.1}{A(\varpi)}\right] \left(\frac{\varpi}{100\ {\rm AU}}\right)^{-1/2} {\rm g\ cm^{-2}}, \quad (64)$$

$$M_d(\varpi) = 4.18 \times 10^{-3} D^{-1} \left(\frac{M_*}{0.5\ M_\odot}\right)^{-1/2} \left(\frac{\dot{M}_d}{2\times 10^{-6}\ M_\odot\ {\rm yr}^{-1}}\right) \times \left(\frac{f}{1-f^2}\right) \left[\frac{0.1}{A(\varpi)}\right] \left(\frac{\varpi}{100\ {\rm AU}}\right)^{3/2} M_\odot, \quad (65)$$

$$\mathcal{J}_d(\varpi) = 0.629 D^{-1} \left(\frac{\dot{M}_d}{2\times 10^{-6}\ M_\odot\ {\rm yr}^{-1}}\right) \times \left(\frac{f^2}{1-f^2}\right) \left[\frac{0.1}{A(\varpi)}\right] \left(\frac{\varpi}{100\ {\rm AU}}\right)^{2} M_\odot\ {\rm km\ s^{-1}\ AU}, \quad (66)$$

$$\nu(\varpi) = 1.81 \times 10^{19} D \left(\frac{M_*}{0.5\ M_\odot}\right)^{1/2} \times \left(\frac{1-f^2}{f}\right) \left[\frac{A(\varpi)}{0.1}\right] \left(\frac{\varpi}{100\ {\rm AU}}\right)^{1/2} {\rm cm^2\ s^{-1}}, \quad (67)$$

$$\eta(\varpi) = 1.56 \times 10^{18} D \left(\frac{M_*}{0.5\ M_\odot}\right)^{1/2} \times \left(\frac{1-f^2}{f}\right) [A(\varpi) 0.1]^2 \left(\frac{\varpi}{100\ {\rm AU}}\right)^{1/2} {\rm cm^2\ s^{-1}}, \quad (68)$$

TABLE 2
PARAMETERS OF FOUR MODEL SYSTEMS

Object (1)	M_* ($M_\odot$) (2)	$\dot{M}_d$ ($M_\odot$ yr^{-1}) (3)	$t_{\rm age}$ (yr) (4)	D (5)	f (6)	$R_\Phi = R_\nu$ (AU) (7)	$M_d(R_\Phi)$ ($M_\odot$) (8)	$\mathcal{J}_d(R_\Phi)$ ($M_\odot$ AU km s^{-1}) (9)	$\lambda(R_\Phi)$ (10)	$Q(R_\Phi)$ (11)
T Tauri star	0.5	1×10^{-8}	3×10^6	$10^{-2.5}$	0.658	298	0.0300	5.12	0.480	4.47
Low-mass protostar	0.5	2×10^{-6}	1×10^5	1	0.957	318	0.200	51.4	3.20	0.381
FU Ori	0.5	2×10^{-4}	1×10^2	1	0.386	16.5	0.0200	0.473	0.320	3.36
High-mass protostar	25	1×10^{-4}	1×10^5	1	0.957	1520	10.0	39700	3.20	0.463

$$\lambda(\varpi) = 0.135 D^{-1/2} \left(\frac{M_*}{0.5\ M_\odot}\right)^{-3/4} \left(\frac{\dot{M}_d}{2 \times 10^{-6}\ M_\odot\ \mathrm{yr}^{-1}}\right)^{1/2} \times \left(\frac{f^{1/2}}{1 - f^2}\right) \left[\frac{0.1}{A(\varpi)}\right]^{1/2} \left(\frac{\varpi}{100\ \mathrm{AU}}\right)^{3/4}, \quad (69)$$

$$\lambda_*(\varpi) = 8.07 D^{1/2} \left(\frac{M_*}{0.5\ M_\odot}\right)^{3/4} \left(\frac{\dot{M}_d}{2 \times 10^{-6}\ M_\odot\ \mathrm{yr}^{-1}}\right)^{-1/2} \times f^{-1/2} \left[\frac{A(\varpi)}{0.1}\right]^{1/2} \left(\frac{\varpi}{100\ \mathrm{AU}}\right)^{-3/4}, \quad (70)$$

$$Q = 56.4 D \left(\frac{M_*}{0.5\ M_\odot}\right)^{3/2} \left(\frac{\dot{M}_d}{2 \times 10^{-6}\ M_\odot\ \mathrm{yr}^{-1}}\right)^{-1} \times \left[\frac{(1 - f^2)^3}{f}\right]^{1/2} \left[\frac{A(\varpi)}{0.1}\right]^{3/2} \left(\frac{\varpi}{100\ \mathrm{AU}}\right)^{-3/2}. \quad (71)$$

3. ASTRONOMICAL EXAMPLES FROM STAR FORMATION

To give astronomical context to the theory developed so far, we consider four examples of interest in current-day star formation: (1) a T Tauri star, (2) an embedded low-mass protostar, (3) an FU Orionis star, and (4) an embedded high-mass protostar. Models 1, 2, and 3 have a central star of mass 0.5 $M_\odot$, and differ only in accreting at rates equal, respectively, to $1 \times 10^{-8}\ M_\odot\ \mathrm{yr}^{-1}$ (Gullbring et al. 1998), $2 \times 10^{-6}\ M_\odot\ \mathrm{yr}^{-1}$ (Young et al. 2003; Young & Evans 2005), and $2 \times 10^{-4}\ M_\odot\ \mathrm{yr}^{-1}$ (see Popham et al. 1996, who, however, have a different explanation for sub-Keplerian rotation near the star than this paper). Model 4, the high-mass protostar, has a mass accretion rate that is scaled relative to model 2, the low-mass protostar, by their masses (see, e.g., Stauber et al. 2007), i.e., both M_* and $\dot{M}_d$ are taken to be a factor of 50 larger. In each YSO disk, we assume a standard flaring law (see, e.g., the dashed curve in Fig. 1*b* of D'Alessio et al. 1999),

$$A(\varpi) = 0.1(\varpi/100\ \mathrm{AU})^{1/4}. \quad (72)$$

We assign $t_{\rm age} = 3 \times 10^6$ yr (Haisch et al. 2001), 1×10^5 yr (Jijina et al. 1999), 100 yr (Herbig 1977), and 1×10^5 yr (Osorio et al. 1999) as the fiducial ages, respectively, of the T Tauri star, low-mass protostar, FU Orionis outburst, and the high-mass protostar. We now compute a viscous-accretion radius R_ν such that $M_d(R_\nu)/\dot{M}_d = t_{\rm age}$. To ensure the approximate validity of the steady-state assumption, we then set $R_\nu = R_\Phi$, where R_Φ is defined as before to equal the radius that contains all the flux, i.e., $\lambda_*(R_\Phi) = \lambda_0$. Since $M_d(R_\nu) = M_d(R_\Phi) = \dot{M}_d t_{\rm age}$ in this formalism, the departure from Keplerian rotation can be computed from equation (60) to equal

$$1 - f^2 = \frac{0.5444 M_*}{\lambda_0^2 \dot{M}_d t_{\rm age}}. \quad (73)$$

For protostars still building up their mass, we expect $\dot{M}_d t_{\rm age}$ to be comparable to M_*. On the other hand, for T Tauri stars or FU Orionis objects, we have $\dot{M}_d t_{\rm age}$ small compared to M_*. Thus, for λ_0 of order 4, we anticipate the departures from Keplerian rotation to be more substantial for T Tauri and FU Orionis stars than for low- or high-mass protostars.

The surface density Σ must drop faster with ϖ than any negative power law in the outer parts of the disk in order to vanish, by definition, at some true outer disk edge R_d. Therefore, unlike the assumption being made at R_ν, the term represented by the right-hand side of equation (3) must change sign in the outermost parts of the disk, leading to a viscous movement outward of R_d with time, carrying to large distances much of the system's angular momentum. Hence, the enclosed angular momentum, calculated from equation (62) with $\varpi = R_\Phi$, may not yield a representative estimate of the system's true total store of angular momentum because it is the least centrally concentrated of the trio: magnetic flux, mass, and angular momentum.

The numerical values of the relevant input parameters are now tabulated in columns (2)–(5) of Table 2; the output bulk parameters from the theory are tabulated in columns (6)–(11). In accordance with the discussion of § 2.3 we have chosen $\lambda_0 = 4$ for all four cases. This choice results in $f = 0.957$ for the low-mass and high-mass protostar models, making magnetocentrifugally driven, cold, disk winds, unassisted by photoevaporation, difficult but not impossible at radii much less than 100 AU for these systems, according to the criterion (31) for appreciable disk winds. If we had chosen a smaller value, say 2, for λ_0, then f would have equaled 0.812, and a powerful disk wind in protostars at any radii other than the inner disk-edge, where magnetospheric interactions dominate, would have been almost as unlikely as the $f = 0.658$ and $f = 0.386$ cases tabulated for the T Tauri stars and FU Orionis systems with $\lambda_0 = 4$.

3.1. *Discussion of Bulk Properties*

In Table 2 we have chosen the numerical value of D to make $R_\Phi = R_\nu \propto D^{4/5}$ reasonable. It is informative in this regard that $D = 1$ works for the two protostar and FU Orionis models (perhaps $D = 0.3$ would be better), but only a relatively small value, $D = 10^{-2.5}$, does as well for the T Tauri model (see, e.g., Andrews & Williams 2007). The enclosed disk mass $M_d(R_\Phi)$ is independent of the numerical value of D, whereas the enclosed angular momentum $\mathcal{J}_d(R_\Phi)$ varies as $D^{2/5}$.

In the case of the FU Orionis model, we are contemplating a *transient* accretion event that has occurred during the past 100 yr and that has swept most of the mass and the magnetic flux to within a radius $\sim R_\Phi = 16.2$ AU, inside of which the system is in quasi–steady outburst. In this case, $R_\nu = R_\Phi$ is likely to be considerably smaller that R_d, where most of the system angular momentum may still reside. In the other cases, we think of $R_\Phi = R_\nu$ as being the effective "outer radius" of the system, large enough to contain the magnetic flux that was dragged into the system by

the star formation process, but small enough so that the available viscosity is able to establish a quasi–steady state if the angular momentum contained in the system is comparable to that tabulated as $\mathcal{J}_d(R_\Phi)$.

Near the disk edge R_d where Σ becomes vanishingly small and B_z matches interstellar values, radial magnetic-buoyancy effects with interchange and/or Parker instabilities may lead to a net loss of flux from the disk. Continuing infall that brings in additional mass and flux from the cloud-core surroundings may counteract such tendencies. Moreover, equations (56) and (57) show that the outer parts of disks contain relatively more mass than flux, so stripping of the outer parts by edge effects, or by tidal encounters with other stars, or by photoevaporation from the far-ultraviolet produced by the most massive cluster members in dense clusters (Adams et al. 2006) cannot do much to alleviate the problem of the growing magnetization of the entire disk. In what follows, we ignore the complications that may arise from all such environmental effects.

One could try to justify very small values of $D = 10^{-3}$ to 10^{-2} in T Tauri models on the basis that only the top and bottom 10 g cm^{-2} of a disk (from ionization by scattered X-rays; see Igea & Glassgold 1999), containing a total Σ of 2000 or 200 g cm^{-2} (which apply roughly at 1 and 5 AU of the "minimum solar nebula"), are active in the accretion process (Gammie 1996). Such small values for the effective D are not out of the question if T Tauri disks have substantial "dead zones" where the ionization is too low to couple to magnetic fields except, possibly, for thin surface layers. The surface density ratio of active zone to dead zone need not be as small as $10^{-2.5}$ (see § 3.2) to result in such a value for D, if accretion in a thin surface layer has an intrinsically smaller efficiency than fully turbulent MRI (see the discussion in § 4.2).

A related problem arises when we apply equation (46) to our T Tauri model, which results in the expression $a \approx 2.64(\varpi/\mathrm{AU})^{-3/8}$ km s^{-1}. An isothermal sound speed of 2.64 km s^{-1} corresponds to a temperature in molecular gas of ~1900 K, a value that is unlikely to hold even in the midplane at 1 AU. The difficulty arises because we took the first term $\propto A$ in equation (46) to be dominant, which requires vigorous inward accretion to sustain the assumed $B_\varpi^+/B_z = I_l = 1.742$ that accounts for the substantial departure from Keplerian rotation $f = 0.658$ computed in Table 2, yet we took the diffusion constant D to equal a paltry $10^{-2.5}$. The inconsistency disappears if we assume that the inner disks of T Tauri stars are dead to the MRI except for their superficial layers. With no magnetic coupling in the deeper layers, f would be much closer to unity in the midplane than indicated in Table 2, and the second term $\propto A^2$ in equation (46) would dominate. We then easily compute that midplane temperatures at 1 AU would be closer to 600 K, and dropping as $(\varpi/\mathrm{AU})^{-1/2}$, more in line with conventional estimates. However, we end with a nonstandard picture in which the central dead layers of T Tauri disks rotate at near-Keplerian speeds, while the active superficial layers tend to be very sub-Keplerian. This picture raises speculative conjectures that we defer to § 4.2.

The enclosed masses $M_d(R_\Phi)$ for the T Tauri and FU Orionis models, which are independent of the choice of effective D (as long as it is a constant as a function of ϖ), are similar to standard estimates. The disk mass of the low-mass protostar is comparable to the masses found by Jørgensen et al. (2007 and references therein) and exceeds a value equal to the "maximum solar nebula" when self-gravitational instabilities would need to be considered (Shu et al. 1990). The disk masses of high-mass protostars are not observationally well studied because of their rarity and consequent larger distances. If the high disk masses for the two

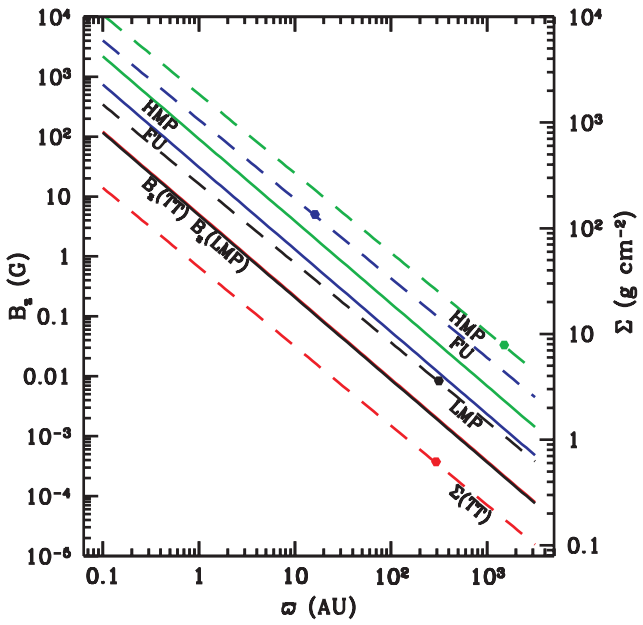

FIG. 2.—Vertical component of the magnetic field B_z (*solid curves*) and the surface density Σ (*dashed curves*) plotted against the radius ϖ in the steady-state disks of the four models of Table 2. The hexagons mark the location where $R_\nu = R_\Phi$ in the T Tauri (*red curves*), low-mass protostar (*black curves*), FU Orionis (*blue curves*), and high-mass protostar (*green curves*) models. The slopes are $-11/8$ and $-3/4$, respectively, for $\log B_z$ and $\log \Sigma$ vs. $\log \varpi$.

protostar models were real, gravitational instabilities could lead to disk fragmentation because $\lambda(R_\Phi)$ and $Q(R_\Phi)$ are, respectively, greater and less than unity in their outer disks.

In contrast, the FU Orionis and T Tauri models are stable to disk fragmentation by both the magnetic and Toomre criteria, $\lambda < 1$ and $Q > 1$. While these conclusions do depend somewhat on the specific choices made for D, the formation of either gaseous giant planets or brown dwarfs by gravitational instability at tens of AU or smaller can probably be ruled out in the model T Tauri system. Thermal cooling is not sufficiently rapid to help (Rafikov 2007). Certainly, close-in brown dwarf companions that could have been easily detected by the Doppler method seem difficult to produce in all our models, which is an after-the-fact explanation for the so-called brown dwarf desert (Marcy & Butler 2000; Halwachs et al. 2000). Our speculations in this regard are consistent with the intuitive notion that large-angular-momentum cases are more prone to making binaries by gravitational fragmentation, whereas small-angular-momentum cases are more prone to making planetary systems by the embryonic core accumulation of solids (Lin 2006).

3.2. *Disk Surface Densities and Magnetic Fields*

Figure 2 shows Σ (in units of g cm^{-2}) and B_z (in units of G), computed from equations (44) and (43), as functions of ϖ (in units of AU) for the four model systems. Hexagons have been placed as stop signs on the formal plots to indicate that the curves for radii larger than $R_\Phi = R_\nu$ should be ignored in any realistic applications. Consistent with Table 2, we have chosen $D = 1$ for the two protostars and FU Orionis, and $D = 10^{-2.5}$ for the T Tauri model.

In the low-mass protostar model, B_z is 302 G, 1.09 G, and 8.74 mG at $\varpi = 0.05$, 3, and 100 AU, respectively, for $D = 1$. In the high-mass protostar model, they are higher by a factor $50^{3/4} = 18.8$ at each radius. The first value in a low-mass protostar, 302 G at 0.05 AU, is compatible with a more-or-less smooth

matching (after enhancement in the X-region) with the inferred field strength of the stellar magnetopause (see Shu et al. 1994), yielding yet another indication why disk truncation occurs inside such radii when the stellar field increases inward much more strongly than the extrapolated disk field.

The second value, 1.09 G at 3 AU, is compatible with the paleomagnetism measured for the chondrules of primitive meteorites, whose parent bodies are believed to originate in the asteroid belt (reviewed by Stacey 1976; Levy & Sonett 1978; Cisowski & Hood 1991). In the X-wind model, whose predictions on this point have received strong support from the recent *Stardust* comet-sample mission (McKeegan 2006; Zolensky et al. 2006), the heating of the chondrule-like materials and refractory inclusions found in meteorites, and now comets, occurs close to the proto-Sun (Shu et al. 1996, 1997). Nevertheless, when ferromagnetic chondrules are thrown out to the asteroid belt, they should not encounter fields that are much stronger than the inferred paleomagnetism result of 1–10 G (Stacey 1976; Levy & Sonett 1978; Cisowski & Hood 1991).

The third value, 8.74 mG at 100 AU, offers an inviting target for Zeeman measurements if appropriate sources of maser emission can be found in protostellar disks. Even more promising for such studies, because maser emission in ringlike configurations has already been found (Hutawarakorn & Cohen 2005; Edris et al. 2007), are the large disk fields predicted for high-mass protostars if their mass accretion rates scale anything like their mass even at radii of a few hundred AU.

Consider now the FU Orionis model. At $\varpi = 0.05$ AU, not far from the putative stellar surface, the vertical magnetic field is predicted to be 1.92 kG if $D = 1$, somewhat higher than the value for $B_z \sim 1$ kG inferred from observations for the inner disk of FU Orionis itself (Donati et al. 2005). A disk that is 4 times thicker, as may happen for the hot inner regions, would eliminate the discrepancy. Moreover, the same observations claim that the inner regions of the disk in FU Ori rotate at a speed 2–3 times lower than the Keplerian value, consistent with $f = 0.386$ in our model. A more detailed study of this system is warranted, but we caution that precise modeling would need to take into account the interaction of the magnetized accretion disk with the (squashed) stellar magnetosphere. If the mass accreted onto the star per FU Orionis event is $M_d(R_\nu) \sim 0.02\ M_\odot$ independent of D, as modeled in Table 2, then it takes tens of such events to accumulate the entire mass of the star, in accord with the astronomical statistics of such objects (Hartmann & Kenyon 1996; but see also Herbig et al. 2003).

Figure 2 shows that the surface densities for the T Tauri model disk are 42.9 and 7.63 g cm^{-2} at 1 and 10 AU, respectively, if $D = 10^{-2.5}$. These are smaller values for the planet formation zones of terrestrial and giant planets than given by conventional minimum solar nebulae (Hayashi et al. 1985) because a comparable disk mass is spread over a much larger area (but see § 4.2). Note that the inferred magnetic field strength at 3 AU is 1.13 G, which is compatible with the chondritic values, and indeed has not changed much from the case of the low-mass protostar. The near equality arises because the low-mass protostar and T Tauri models have about the same flux and the same radius, although their disk masses differ by a factor of 6.67 and their angular momenta by a factor of 10 (for the chosen values of D). Thus, Figure 2 shows that the surface densities differ by a factor of a little over 6, but the two B_z curves lie almost on top of one another all the way out to about the same position for the two hexagons. This result makes graphic the point that the T Tauri disk rotates slower than the low-mass protostar disk because the former is more strongly magnetized relative to the disk mass. Indeed, one could heuristically imagine the low-mass protostar evolving into the T Tauri system if the excess mass and excess angular momentum could be put into an orbiting stellar companion without changing the magnetic flux distribution.

With D equal to a strict constant, the surface densities corresponding to low, typical, and high power-law flaring, $A(\varpi) \propto \varpi^{1/8}$, $\varpi^{1/4}$, and $\varpi^{1/2}$, are respectively $\Sigma \propto \varpi^{-5/8}$, $\varpi^{-3/4}$, and ϖ^{-1}, consistent with the power-law range deduced from the thermal dust-emission of YSO disks (Andrews & Williams 2007), but shallower than some of those inferred from CO brightness as reviewed by Dutrey et al. (2007) or the law $\Sigma \propto \varpi^{-3/2}$ associated with conventional minimum solar nebulae (Hayashi et al. 1985). However, for T Tauri stars, once one allows the possibility that D might be substantially smaller than unity because of physical considerations other than fully developed MRI turbulence (see below), then there is no reason to think that D would be a spatial constant. On the other hand, we may do well to recall that the steeper, empirical, log-log slope is derived from the inferred distribution of solids, which may, as seems to be implied by the comet Wild results (McKeegan 2006; Zolensky et al. 2006), have been affected relative to the gas by the recycling of rock from the hot disk regions near the proto-Sun to the rest of the solar nebula, as well as by the migration of planets. In any case, we would be the first to admit that our models do not allow for a straightforward recovery of models that look like the "minimum solar nebula." Probably no viscous accretion disk can "succeed" in this regard (see Fromang et al. 2002).

Vorobyov & Basu (2006) suggest that FU Orionis outbursts are associated with spiral gravitational instabilities in a protostellar disk. We are sympathetic to the view that such self-gravitational disturbances can play a role in the early evolution of protostars that are still in the main infall stage that builds up the final system mass (Shu et al. 1990). We are, however, agnostic when it comes to the issue of whether FU Orionis systems represent such early-stage objects or not. Accurate estimates of the outburst disk masses in FU Orionis systems—whether they are closer to "minimum" or "maximum" values—can prove to be observationally decisive in this debate.

4. HIGH AND LOW STATES OF ACCRETION

In § 3 we have presented the astrophysical case that there are high states of accretion where D is of order unity (FU Ori, low- and high-mass protostars) and low states where D is much less than unity (T Tauri stars). Indeed, even low-mass protostars (or, at least, the so-called Class I sources) may alternate between high- and low-states of mass accretion (White et al. 2007). In § 4.1 we speculate that the MRI is fully developed in high states, and we consider mechanisms that may allow turbulent values of ν and η, in a situation with dynamically strong mean fields, to achieve the saturated ratio of equation (24) in steady state. Likewise, in § 4.2 we discuss the weak-turbulence conditions likely to prevail on scales smaller than a vertical scale height z_0 in low states, focusing in particular on the form of MRI likely to be present when dead zones are bottlenecks to rapid disk accretion, with the activity being concentrated in thin surface layers (Gammie 1996).

4.1. *Magnetic Loops and Their Dynamics*

To picture how rapid transport of matter and magnetic fluctuations across strong mean field lines that are anchored externally is possible, we adopt a mental image of field loops on a scale smaller than z_0. This mental image can be given a physical correspondence in the equations of magnetohydrodynamics in axial symmetry, but the task becomes much harder if the current

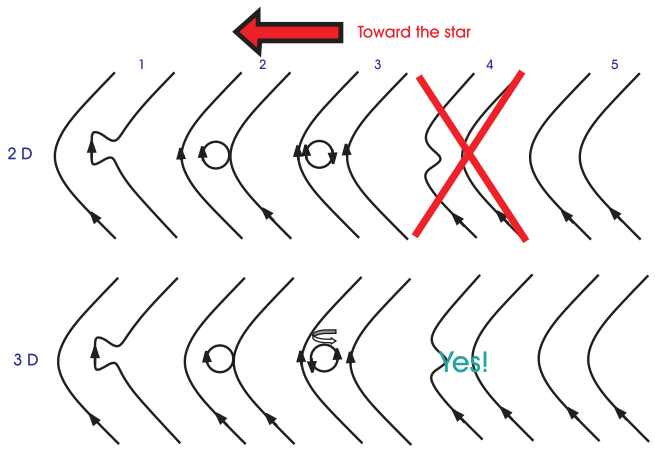

FIG. 3.—Schematic diagram of scenarios by which field loops are created by magnetohydrodynamic turbulence when the mean field is strong: in 2D by stretch, pinch, disconnect (*top*) and in 3D by stretch, pinch, disconnect and twist, reconnect, relax (*bottom*). The depiction is the meridional plane (ϖ, z), except for the twist indicated by the block arrow, which occurs out of the plane of the paper in the φ-direction because of differential rotation. Note the bias for forming the loop on the side closer to the star because of the accretion flow. This bias causes the diffusive flux to flow in the correct direction relative to the curl of mean $\boldsymbol{B}$. Because the loop in the top diagram does not experience the twist operation, it has the wrong orientation to reconnect with the mean field downstream of the mean accretion flow since the fields point up on both sides of the target contact point. The twist in the bottom diagram gets the fields oriented in opposite directions at the target reconnection point, which results in the green "yes" sign to proceed to steps 4 and 5.

associated with the loop has structure in the φ-direction. We ignore this complication in the heuristic discussion based on a diagram (Fig. 3) that shows only one field loop, born of a single mean field line, that has complete freedom to move as if there were no constraints from neighboring field lines and other loops. Because we make no attempt to be quantitative except for a single order-of-magnitude calculation, this mental image can suggest possible interpretations without misrepresenting, hopefully, the complex, nonlinear dynamics of fully developed, 3D MRI turbulence.

Consider a process that bends, pinches, and twists a field line into a loop that eventually disconnects from its parent field line by resistive dissipation (bottom set of diagrams in Fig. 3). The loop is then advected to the next set of field lines, to which it reconnects, relaxes, and gets into position to form another loop. To visualize what is happening in this figure, recall that magnetic field lines never end, but are directed continuously from point to point on a given line, except during reconnection, when oppositely directed fields can annihilate, leaving the remaining fragments to join up in a new field-line configuration. In a random field of fluid turbulence with a straight and uniform distribution of the mean field, a loop is as likely to get transported away from the star as toward it; i.e., the loops do a random walk, and the entire process is describable as a "diffusion" across mean field lines. The process has directionality and becomes a diffusive flux when the mean field has a spatial curl defined by the mean accretion flow, as drawn in the diagram.

Note that the entire"bend-pinch-disconnect and twist-reconnect" process requires helical turbulence in three dimensions, with differential rotation providing the critical "twist" part of the process. Similar diagrams were drawn by Parker (1955) in his famous proposal for the mechanism of dynamo action. In the present context, the "twist" also implies an outward transport of angular momentum if it is accompanied by the shearing of the radial field B_ϖ to give an azimuthal component B_φ. In this manner, the entire sequence of steps provides both an effective viscosity for angular momentum transport and an effective resistivity for matter to move from one set of field lines to another. In 2D, "bend-pinch-disconnect" gives a loop that can transport angular momentum if the shear of differential rotation generates a B_φ from the local B_ϖ (a "2.5D" process). But the loop, without an additional vortical "twist" in the third direction (requiring an "eddy" motion out of the page, azimuthally in the drawing), has the wrong orientation to attach to the next set of mean field lines (top set of diagrams in Fig. 3 with the fourth "reconnect" step forbidden by the large red cross). Thus, the loop will be trapped between the thicket of nonzero mean field lines, and it will eventually retrace steps 3-2-1 and merge back onto the original field line (or with other loops carrying the same sense of current), causing the matter to become reattached more or less to the same field location except for the slight diffusion associated with dissipation by the microscopic collisional resistivity. In such a situation, the fluctuations associated with MHD turbulence are probably better described as a random collection of Alfvén waves rather than as a diffusing, merging, set of magnetic loops.

The 3D process appears in many MRI simulations when the plasma β is large compared to unity ($\sim$100; see Appendix B). It remains to be seen whether it persists in the presence of a mean field as dynamically strong as we advocate in this paper. In any case, the random walk of magnetic loops, carrying an associated current, can move through the thicket of mean field lines faster than individual particles or particulates can get knocked off one set of field lines by physical collisions to attach onto the next set of field lines, allowing for "viscous" and "resistive" diffusivities that are larger than conventional microscopic values. The magnetic dissipation process is sometimes described by *hyperresistivity*, i.e., turbulent transport of current, not field, which was originally proposed to describe magnetic relaxation in plasmas (Strauss 1976; Diamond & Malkov 2003). Appendix A shows how the simplest mathematical model of a diffusion of φ-current rather than a diffusion of z-field yields the same practical results as § 2, but with a Prandtl ratio $\eta_J/\nu \sim 1$ rather than $\eta/\nu \ll 1$.

In a pure-loop picture, the derivation of § 2.1 really applies then to the loop dynamics of Figure 3. In other words, B_ϖ of that derivation is really δB_ϖ of the loop, with the change in sign of δB_ϖ from the top to the bottom of the loop being irrelevant because the δB_ϕ that is produced by shearing will have the correct compensating sign as already noted in the discussion of § 2.1. We then assume $\delta B_\varpi \sim B_\varpi^+$ and $\delta u \delta B_\varphi \sim \varpi(d\Omega/d\varpi)\delta\varpi\delta B_\varpi$, with the corresponding Maxwell stress calculated from the quadratic correlation of $\delta B_\varpi \delta B_\varphi$ assuming $\delta u \sim \Omega\delta\varpi$ as in § 2.1. The estimate for ν then goes through as before, with the large uncertainties in proportionality constants absorbed in $\mathcal{F}$ and eventually D. Consistent with the discussion of the formulation of the mean field MHD equations in § 1.1, we then have a mathematical separation in which there is no mean B_φ when averaged over z, but there are local fluctuations δB_φ whose correlations with δB_ϖ do not average to zero.

The estimate for $\eta \sim A\nu$ with $A = z_0/\varpi \ll 1$ might follow because all detached and nondetached loops can transport angular momentum but only a fraction of the detached ones have the right geometry and orientation to reconnect with mean downstream field lines, yielding an effective resistivity η that is much smaller than the turbulent viscosity ν. The exact relation (24), which includes an extra factor of $3/2I_l$, then presumably arises because, in steady state, the rotation law is quasi-Keplerian and the surface density has a power-law index $-2l$ (eq. [22]). The fact that the scale of the turbulent mixing length $\delta\varpi$ was left unspecified in § 2.1 (in actuality, a spectrum of such scales and shapes) may give the problem the necessary degree of freedom

to make matters come out exactly right. At some basic level, the macrophysics of fully developed MRI makes angular momentum transport the driving energy-release mechanism behind the inward fluid drift in disk accretion. The formation rate, merger rate, and geometry of magnetic loops may be regulated to yield a turbulent resistivity, $\eta = (3A/2I_l)\nu$, that is well below the naive Prandtl ratio $\eta \approx \nu$ because no energy source exists to cause gas to diffuse across flux tubes faster than the saturated value. Conversely, if η were to fall below the level $(3A/2I_l)\nu$, the resultant pileup of mean field lines waiting to diffuse inward (see LPP94, whose solution for the induction equation remains valid independent of any implicit or explicit assumptions about Ω) would presumably cause a shift in the numbers and kinds of loops generated until η approaches the saturated level. However, more rigorous theoretical studies and/or numerical simulations are needed if we are to gain confidence that MRI dynamics under the circumstances envisaged in this paper can truly satisfy the diffusivity-ratio constraint implied by equation (24) with ν given by equation (42). If such studies show that equation (24) cannot be achieved, then a possible resolution for real systems is to alternate between trying to satisfy $u = -3\nu/2\varpi$ and $u = -(\eta/z_0)B_\varpi^+/B_z$, making relaxation oscillations between the two conditions the real cause of low states and high states, with FU Orionis outbursts and their decay as the transition phenomenon.

In our enthusiasm for magnetic loops, we should not forget that Alfvén waves can also carry angular momentum, depositing it in the matter when they dissipate. If the MRI is operating at maximum efficiency, it is easy to show that the frequency associated with Alfvén waves of wavenumber scale z_0^{-1} is comparable to Ω. For larger wavenumbers (smaller scales), the Alfvén wave frequency is larger than the natural eddy turnover frequency Ω, leading us to a picture of the generation of Alfvén waves by the bending or twisting of protoloops of scale z_0 that do not detach from their mean field lines, before these wavelike disturbances propagate, go into a free cascade, and dissipate from interactions of the type described by Goldreich & Sridhar's (1997) theory of MHD turbulence. It is unlikely that the competition with loop detachment and merging from such wave-transport effects could be adequately described by diffusion equations at a macro level.

4.2. *Two-dimensional MHD Turbulence and Layered Accretion*

Creating loops of field and chopping them off from mean field lines by turbulent fluid motions may not be possible when the coupling to magnetic fields is weak, and the MRI transport mechanism becomes confined to surface layers where the ionization level is still sufficiently high (the situation in T Tauri disks). The formation of the loops themselves becomes difficult because the restricted height practically available for z-motions may make the fluid effectively two-dimensional. In particular, lifting parcels of gas against their own weight in the z-direction either to bend field lines or to twist them, added to the energy needed to stretch and pinch magnetic fields, may prove relatively difficult in thin surface layers compared to the same processes near the midplane where the vertical gravity vanishes. In other words, the MRI is an intrinsically 3D instability, and it cannot operate efficiently in a 2D magnetofluid except as artificial "channel flows" (see, e.g., Goodman & Xu 1994) where the following considerations still apply.

In circumstances where the flow is confined to 2D, the turbulent resistivity η is "quenched," becoming proportional to its microscopic collisional value, although enhanced by a factor $(\delta B/B)^2$ when the fluctuations are large (Cattaneo & Vainshtein 1991; Gruzinov & Diamond 1994, 1996; Diamond et al. 2005). No matter how intricately turbulence distorts magnetic field lines in the remaining two (horizontal) directions, electrically conducting particles cannot get off the field lines about which they gyrate, unless they are knocked off by microscopic physical collisions. In 2D MHD turbulence, an inverse cascade of squared magnetic potential exists alongside the familiar energy cascade to smaller scales. This inverse cascade reflects a competition between the tendencies of velocity fluctuations to chop up isocontours of magnetic potential, thus producing smaller scales, and of magnetic loops to aggregate because of the attractive force between parallel lines of current, thus producing larger scales. Thus, field lines never get chopped up systematically into small loops that can be reconnected much more quickly than the laminar dissipation of the mean fields. In layered accretion, therefore, the transport of mass and angular momentum are subordinate to the diffusion of field, and the effective turbulent ν in the active surface layers may be constrained to be compatible with the microscopic collisional value of η. Because the entire layer is not involved in the relevant diffusive processes, a formulation that integrates through the vertical thickness cannot do justice to the real problem, which has a bimodal vertical stratification.

At a minimum, we should consider instead a two-layer description and introduce surface densities Σ_s and Σ_m that describe respectively the columns through the upper and lower (active or live) surface layers and a middle (inactive or dead) layer, which sum to the total Σ of the current formulation. In this picture, the values cited for the surface densities and magnetic field strengths in § 3.2 probably refer more to the active layer than they do to the total. Although the layer thickness expressed in terms of Σ_s may be more-or-less fixed by the (external) sources of ionization, the magnetic field strength B_z is potentially adjustable as a function of ϖ to give a constant accretion rate $\dot{M}_d$ in steady state, which yields an advantage of such a description of layered accretion over that given originally by Gammie (1996).

Our current calculations yield no constraint on the possible surface density of the inactive layer Σ_m. Magnetic fields have freedom to move with respect to the nearly unionized gas in Σ_m that rotates at near Keplerian speeds. Shear instabilities arising from upper and lower surfaces that rotate slower than the midplane layers could lead to breaking radial buoyancy waves that provide torques to redistribute the angular momentum of the "dead gas" (Vishniac & Diamond 1989). The coupling provided by the excitation of waves in dead zones has been explicitly demonstrated in the simulations by Fleming & Stone (2003) and Wünsch et al. (2006). In a more simplified approach that would not attempt to resolve the internal structure of the upper and lower layers, the layer with surface density Σ_s, would be described by the equations given in this paper, except again for a frictional term coupling them to Σ_m. With Σ_m included as a frictional load, the net effect would be as a variable D in the single-layer description of the total surface density Σ. In other words, ν is slaved to η in Σ_s in the active, but geometrically thin, surface layers, and η is given by its collisional value. Then D is simply a defined quantity in the current formula (42) for the relationship between ν, B_z, z_0, Ω, and *total* Σ. Such a two-layer model, with enough microphysics to specify the collisional value of η in a complex, dusty, plasma, would allow us to calculate the variation of the effective D with ϖ in our current one-layer description.

Figure 4 gives the estimate by Sano et al. (2000) of the microscopic collisional value of η in the midplane of a Hayashi model solar nebula with dust of unagglomerated interstellar size and ionized by Galactic cosmic rays. The collisional resistivity in the inner disk ($\varpi < 3$ AU) is consistent with the magnitude

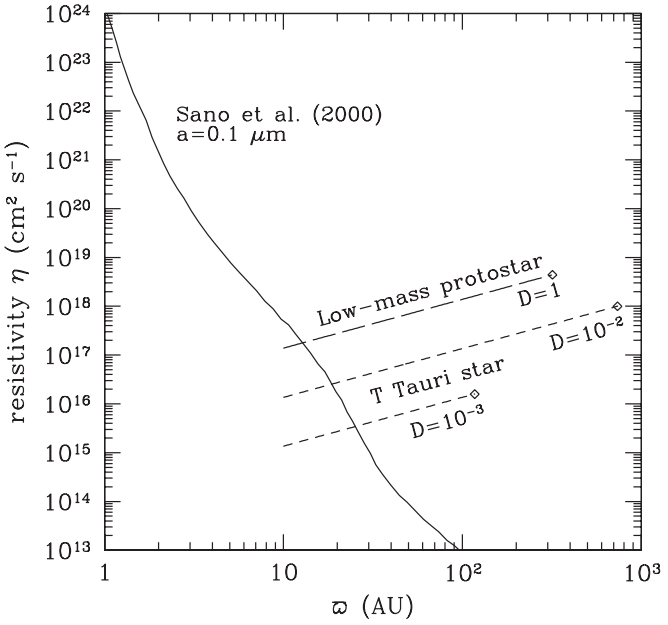

FIG. 4.—Comparison of collisional resistivity (*solid curve*) applicable to the Sano et al. (2000) model of the minimum solar nebula, which includes the effects of cosmic grains of typical interstellar size ($a = 0.1$ μm) with the required turbulent values in the models of § 3 of a low-mass protostar (*long-dashed line*) with $D = 1$ and a T Tauri star (*short-dashed lines*) with $D = 10^{-2}$ (*top*) and $D = 10^{-3}$ (*bottom*). The hexagons mark the corresponding locations of $R_\oplus$ where the disk holds the trapped flux corresponding to a dimensionless mass-to-flux ratio $\lambda_0 = 4$.

$\sim 10^{20}$ cm^2 s^{-1} cited by Shu et al. (2006) as needed for dynamic disk formation. The collisional resistivity beyond $\sim$10–20 AU is lower than the values needed for the low-mass protostar model (*long-dashed line with* $D = 1$) or for the T Tauri model (*short-dashed lines with* $D = 10^{-2}$ *and* $D = 10^{-3}$). In the interpretation of this section, then, once disk formation has occurred, its accretion resistivity would need to arise from MRI turbulence at large radii, whereas interior to 10–20 AU, dead zones may be present and collisional resistivities may be adequate for the needed field diffusion even in the thin surface layers where viscous accretion is active.

An interesting question then arises as to what can initiate a transition between a low state and a high state of accretion. It is natural to expect the transition to originate at a boundary between dead zones and live zones. By definition, such boundaries are not thin layers in any description where vertical stratification matters. The electric fields experienced by charged particles forced by collisions to rotate in the dead zone relative to the magnetic field, at speeds characterizing the large slip between the magnetically coupled active layer Σ_s and the magnetically decoupled layer Σ_m, may generate suprathermal particles. These suprathermal particles might produce the ionization that converts Σ_m into a better conducting medium. Unfortunately, the existing numerical simulations of dead zones do not help us much in the latter regard because the acceleration of suprathermal particles requires a kinetic treatment, not just a (magneto)hydrodynamic one. Moreover, the large slip is missing in the local simulations of Fleming & Stone (2003), and the magnetic field is missing in the global simulations of Wünsch et al. (2006). Heating by the resulting enhanced accretion may further enhance the development of the three-dimensional turbulence of the type with which we started the discussion of this section. The boundary would then eat its way radially into the zones that were previously dead. An interesting theoretical goal would be to see how this transition between low states and high states works in detail and whether an FU Orionis outburst begins inside-out or outside-in since sufficiently ionized regions from conventional sources exist on both sides of normal dead zones.

5. SUMMARY AND CONCLUSIONS

The discussion of § 4 represents our attempt to resolve the conflicts imposed by the following separate issues:

1. the existence of a definite relationship between ν and η in steady state,
2. the evidence that the common diffusion coefficient D has a value of order unity in some systems and much less than unity in others,
3. the fact that MHD turbulence has a very different character in 2D compared to 3D,
4. the suggestion that η may be limited to have essentially its microscopic collisional value in layered accretion, and
5. the difficulty of weak magnetic coupling when "dead zones" arise in YSO disks.

Our suggestions in § 4 are therefore as much a road map of needed future research as they are a catalog of the mysteries of the present and the past.

In retrospect, the biggest mystery concerns the most observationally well studied disks associated with star formation, those in T Tauri systems. We may phrase the conundrum as follows. Diffusive processes cannot remove angular momentum or magnetic flux from the system; they can only redistribute them within the system. In a closed system, T Tauri stars represent an end game for viscous resistive disks whose mass steadily drains into the central star, but whose magnetic flux and angular momentum, inherited by gravitational collapse from the interstellar medium, remain more-or-less trapped in the surrounding disk. Such a situation must result eventually in a magnetically dominated disk. To prevent the residual disk from spreading to very large radii in a fixed amount of time, then, demands inefficient diffusion (small D). The astronomical challenge therefore becomes to explain why there are two physical states of accretion, an active state (protostars, FU Orionis outbursts), characterized by a D with a more "natural" value $\sim$1, and an inactive state (T Tauri stars), characterized by a $D \ll 1$.

The conventional assessment is that "dead zones" provide the resolution for why the mass accretion rate is so low in T Tauri disks observationally, or why the effective $D \ll 1$ in our language. But if this is the correct answer, then why should D ever be as large as unity in other contexts, the most obvious being FU Orionis outbursts? These disks have even higher column densities of disk matter that can shield external sources of ionization, principally, X-rays and cosmic-rays. Why are they not even more full of dead zones? We have proposed exploring the possibility that the high states of disk accretion correspond to the removal of such barriers. Perhaps a fraction of the energy released in the resistive dissipation of stressed fields accelerates suprathermal particles and thus provides a level of in situ ionization much in excess of the sources considered in conventional solar nebula models. Thus, the MRI mechanism, properly generalized to include the dissipation of currents generated by the stressing of mean fields from viscous accretion, may contain its own solution to the challenge posed by low ionization (see also Fromang et al. 2002). Heating from enhanced accretion may also help with the ionization of trace species such as lithium and potassium. Indeed, since any bootstrap mechanism allows the potential of a runaway—more ionization →

more coupling → more ionization, etc.—this proposal also offers an opportunity, perhaps, to understand why disk accretion in YSOs can alternate between low and high states of accretion, characterized generically by T Tauri stars and FU Orionis outbursts.

The complementary difficulties noted above are related to a serious problem noticed by King et al. (2007). The effective α_{ss} in a Shakura-Sunyaev prescription for disk viscosity has to be of order 0.1–0.4 to explain the empirical facts known about thin, fully ionized, accretion disks in many astronomical contexts, yet the equivalent α from almost all MRI simulations to date is lower typically by 1 or more orders of magnitude (e.g., as summarized by Gammie & Johnson 2005 and modeled by Fromang et al. 2002). By coincidence, low values for $\alpha_{ss} \sim 10^{-2}$ are empirically acceptable for modeling T Tauri disks (see, e.g., Hartmann et al. 1998), because such disks have extensive dead zones in which only a small fraction of the total surface density is actively accreting. But if the estimates from MRI simulations were applied only to the active layers, the net effective value of α_{ss} (in the sense of a combined two-layer model) would have been more like 10^{-4} than 10^{-2}.

Among the possible resolutions mentioned by King et al. (2007) are stronger magnetic fields and global rather than local simulations for the MRI that occurs in realistic systems. The results of the present paper (see especially the discussion of §§ 2.1 and 4.1) strongly support such a resolution of the existing paradox, at least for the field of star formation. Most MRI simulations ignore the presence of a nonzero magnetic flux that threads through the disk, carried in by the process of gravitational collapse. As demonstrated in this paper, the presence of an externally supplied magnetic field makes the self-consistent dynamics considerably more subtle than the simplest notion of the MRI extant in the literature. In particular, the accretion flow generates, on either side of the midplane, a mean radial field B_ϖ from the mean vertical field B_z because of the inward drift and the imperfect tendency toward field freezing. This mean radial field, whose surface value is denoted by the symbol B_ϖ^+ in this paper and whose properties can be deduced only by a global calculation that takes proper consideration of the vacuum conditions above (and below) the plane of the disk, sets the scale for turbulent fluctuations (if MRI arises) and has three important consequences.

First, as emphasized in § 4.1, the resultant poloidal-field configuration can spawn magnetic loops, possessing a radial component of the magnetic field δB_ϖ whose amplitude is proportional to B_ϖ^+. The loop can be stretched in the azimuthal direction by the differential rotation in the disk to produce an azimuthal field δB_φ that has a systematic orientation with respect to δB_ϖ. The correlation of δB_ϖ and δB_φ then exerts a Maxwell stress much larger than the corresponding values obtained in simulations of MRI where there is no external field B_z to set a scale for B_ϖ^+. The Maxwell stress leads to angular momentum transport that yields the original accretion responsible for the generation of mean B_ϖ^+ from mean B_z.

Second, the resultant poloidal-field configuration introduces current flows that can be dissipated by resistive effects. An important finding of our study, extending the work of LPP94, is that the ratio of the effective resistivity η to the turbulent viscosity ν must have a well-specified value in steady state that depends on the local aspect ratio of the disk (vertical thickness to radius). The exploration of the implications of this result for the turbulent microphysics of the problem, in particular, how the microscopic dynamics of the current loops can automatically adjust to the requirements of the macroscopic problem, needs further theoretical study, best supplemented by numerical simulation.

Third, the resultant poloidal-field configuration produces a change in the radial force balance, giving a deviation from the traditionally invoked Keplerian profile. This deviation is not easily detectable observationally because the resulting rotation law has in steady state the same power-law dependence with radius as a true Kepler law, but the coefficient is smaller. Thus, even if it were present, observers would tend to attribute the result to the mass of the central object being smaller than its actual value, or to the disk being inclined by a lesser amount than in reality. Nevertheless, it would be illuminating to find such an effect in the YSO disks that have the smallest mass-to-flux ratios. Indeed, a deduction of sub-Keplerian rotation of the disk may already have been made in the case of FU Orionis (Donati et al. 2005), but the proper interpretation of the phenomenon in this case may be complicated by the interaction of the disk field with the imperfectly squashed stellar fields of the central object. Finally, it has not escaped our attention that significant departures from true Keplerian rotation of a YSO disk may have important consequences for the problems of binary-star and planetary-system formation and evolution, particularly with regard to the difficult issues of orbit migration and eccentricity pumping (e.g., Sari & Goldreich 2004). The inward drift of solids from sub-Keplerian regions into the dead zones of the problem, which rotate more nearly at Keplerian speeds, may give an additional reason to focus on the importance of dead zones for the problems of planetesimal and planet formation (e.g., Youdin & Shu 2002; Pudritz & Matsumura 2004).

We thank Steve Lubow for pointing us to the paper by Ogilvie (1997). F. S. is grateful for the support of the UCSD physics department; D. G. and S. L. wish to thank the Astronomy Department of the University of California at Berkeley for hospitality. S. L. also acknowledges support from CONACyT 48901 and PAPIIT-UNAM IN106107; A. G., from NSF grant AST 05-07423; and P. D., from US Department of Energy grant FG02-04ER 54738.

APPENDIX A

ALTERNATIVE FORMULATIONS FOR TURBULENT DIFFUSION

A turbulent, magnetized medium may not behave in the assumed model fashion, with diffusive fluxes proportional to a scalar diffusivity times the rate of spatial variation of the mean quantity that is being spread (Fick's law). For example, Pessah et al. (2006) perform a quasi-linear analysis of the MRI with third-order closure in a simple shearing-box geometry. They claim that the turbulent viscous stress $\Pi_{\varpi\varphi}$ depends on the rate of shear by a non-Fickian power p that is different from 1. If we denote $(\varpi/\Omega)\partial\Omega/\partial\varpi$ by $-S$, then their model yields $\Pi_{\varpi\varphi} = -\hat{\nu}\Sigma\Omega S^p$ with p between 3 and 4. However, *in a field of quasi-Keplerian rotation* where $\Omega \propto \varpi^{-3/2}$, S is simply the number 3/2. Thus, the Pessah et al. formalism satisfies, in practice, the usual Newtonian relationship, $\Pi_{\varpi\varphi} = \nu\Sigma\varpi\partial\Omega/\partial\varpi$, where $\nu = (3/2)^{p-1}\hat{\nu}$. This simple transformation allows the translation of all of our results into the language of Pessah et al.

A similar remark applies to the induction equation (4). Instead of the diffusion of vertical field, some mean field formulations of turbulent MHD (see § 4.1) envisage the diffusion of tangential current (per unit length). From Ampere's law, $J_\varphi = (c/2\pi)B_\varpi^+$, and the

TABLE 3
ESTIMATES OF D

Run	$\beta(0)$	$\langle\langle B_x B_y\rangle\rangle/\langle\langle B^2\rangle\rangle$	$\langle\langle B^2\rangle\rangle/\langle\langle B_z^2\rangle\rangle$	D
S96 IZ1	100	0.145	26.7	0.2
S96 IZ3	25	0.139	...	...
MS00 ZN2	100	0.0716/0.0958	...	...
MS00 ZN1	25	0.0111/0.00586	40/26	0.03/0.01

diffusion of mean current is equivalent to the diffusion of the mean radial field. Then, instead of equation (4), we might postulate a diffusion equation of the form

$$\frac{\partial B_\varpi^+}{\partial t} + \frac{1}{\varpi}\frac{\partial}{\partial \varpi}\left(\varpi B_\varpi^+ u\right) = \frac{1}{\varpi}\frac{\partial}{\partial \varpi}\left(\eta_J \varpi \frac{\partial B_\varpi^+}{\partial \varpi}\right), \tag{A1}$$

where η_J is the diffusivity for the turbulent diffusion of current. In steady state, radial force balance in a field of quasi-Keplerian rotation will still require $B_\varpi^+ = I_l B_z \propto \varpi^{-(5+2n)/4}$ (see §§ 1.3 and 2). In this case, the above equation is equivalent to equation (4) if we identify

$$\eta_J = \frac{4 I_l}{(5+2n)}\left(\frac{\eta}{z_0/\varpi}\right) = \left(\frac{6}{5+2n}\right)\nu, \tag{A2}$$

where we have used equation (24). For $n = 1/4$, the relationship between η_J and ν is then $\eta_J = 1.09\,\nu$, a result that we might call the "Prandtl hypothesis" because it differs only slightly from the naive guess that diffusion processes in a turbulent medium have equal steady-state diffusivities (see the discussion in LPP94). Thus, what seems more relevant than the specific turbulent diffusivities are the turbulent fluxes, and how those fluxes relate to the spatial derivatives of mean-flow quantities.

APPENDIX B

THE VALUE OF D FROM MRI SIMULATIONS

In Table 3, we list the ratio of magnetic stress to magnetic energy density from Table 1 of Stone et al. (1996, hereafter S96) and from Table 1 of Miller & Stone (2000, hereafter MS00). Double angle brackets indicate time and volume averages (mostly over 2 scale heights) for the two smallest values of the initial midplane β-parameter, $\beta(0)$, in these papers. S96 use periodic boundary conditions in all three directions and a vertical box height 3 times the initial pressure scale height H. MS00 employ an outgoing boundary condition at the top of a box of height $5H$. In the table, two averages are included for the results of MS00, which apply to the regions $|z| < 2H$ (fourth row) and $|z| > 2H$ (fifth row). Empty entries occur when the required information is not given in the original papers.

In the simulations, B_x and B_y contain only fluctuating components, whereas B_z and total B contain both mean and fluctuating components, with the mean components being systematically destroyed by numerical reconnection as the simulations proceed because the starting distribution of B_z alternates in sign radially. If we equate the tangential Maxwell stress per unit circumferential length (which dominates the corresponding expressions for the Reynolds stress) to an equivalent viscous stress in the usual manner, we obtain the following expression for ν for the case of quasi-Keplerian rotation:

$$\nu = \frac{z_0}{3\pi\Sigma\Omega}\langle\langle B_x B_y\rangle\rangle. \tag{B1}$$

Introducing a factor of $\langle\langle B^2\rangle\rangle$ on top and bottom to express the relevant ratios in the form of Table 3, we can now identify the coefficient D in equation (42) as

$$D = \frac{1}{6\pi}\frac{\langle\langle B_x B_y\rangle\rangle}{\langle\langle B^2\rangle\rangle}\frac{\langle\langle B^2\rangle\rangle}{\langle\langle B_z^2\rangle\rangle}. \tag{B2}$$

The results in Table 3 give values of D that differ by an order of magnitude, indicating that the MRI simulations are sensitive to the assumed boundary conditions and to the size of the computational box. As a formal result, the last column of Table 3 seems to suggest that D is, at best, 0.2. However, as emphasized in the text, simulations with net magnetic flux equal to zero do not correspond to the situation of interest for our study.

APPENDIX C

VERTICAL STRUCTURE OF STRONGLY MAGNETIZED DISKS

Inside a thin disk, the condition of vertical hydrostatic equilibrium reads

$$\frac{\partial}{\partial z}\left(P + \frac{B_\varpi^2 + B_z^2}{8\pi}\right) = -\frac{G M_* z \rho}{\varpi^3}, \tag{C1}$$

where P is the thermal gas pressure and B_ϖ is a function of z equal to 0 at $z = 0$ and to B_ϖ^+ at the disk's surface, whereas B_z may be taken to be a constant over the same range of z. If we integrate equation (C1) from $z = 0$ to the surface under the boundary conditions that $P(0) = a^2\Sigma/2z_0$ (which defines what we mean by a^2) and $P = 0$ at the disk's surface (which defines what we mean by the surface), we get

$$\frac{I_l^2 B_z^2}{8\pi} - \frac{a^2\Sigma}{2z_0} = -\frac{GM_*\Sigma z_0}{4\varpi^3}, \tag{C2}$$

where we have defined z_0 by requiring the integral of $z\rho$ from $z = 0$ to the surface of the disk yield $(z_0/2)(\Sigma/2)$. With $B_\varpi^+ = I_l B_z$, the equation of radial force balance (eq. [18]) reads

$$\frac{I_l B_z^2}{2\pi\Sigma} = (1 - f^2)\frac{GM_*}{\varpi^2}. \tag{C3}$$

Elimination of B_z^2 from equations (C2) and (C3), with $z_0 = A\varpi$, then gives equation (46).

REFERENCES

Adams, F. C., Proszkow, E. M., Fatuzzo, M., & Myers, P. C. 2006, ApJ, 641, 504
Andrews, S. M., & Williams, J. P. 2007, ApJ, 659, 705
Bachiller, R. 1996, ARA&A, 34, 111
Balbus, S. A., & Hawley, J. F. 1998, Rev. Mod. Phys., 70, 1
Basu, S., & Mouschovias, T. Ch. 1994, ApJ, 432, 720
Binney, J., & Tremaine, S. 1987, Galactic Dynamics (Princeton: Princeton Univ. Press)
Blandford, R. D., & Payne, D. G. 1982, MNRAS, 199, 883
Cattaneo, F., & Vainshtein, S. I. 1991, ApJ, 376, L21
Chan, K. L., & Henriksen, R. N. 1980, ApJ, 241, 534
Cisowski, S. M., & Hood, L. L. 1991, in The Sun in Time, ed. C. P. Sonett, M. S. Giampapa, & M. S. Matthews (Tucson: Univ. Arizona Press), 761
D'Alessio, P., Calvet, N., Hartmann, L., Lizano, S., & Canto, J. 1999, ApJ, 527, 893
Diamond, P. H., Hughes, D. W., & Kim, E. 2005, in Fluid Dynamics and Dynamos in Astrophysics and Geophysics, ed. A. Soward, C. Jones, D. Hughes, & N. Weiss (Boca Raton: CRC Press), 145
Diamond, P. H., & Malkov, M. 2003, Phys. Plasmas, 10, 2322
Donati, J. F., Paletou, F., Bouvier, J., & Ferreira, J. 2005, Nature, 438, 466
Dutrey, A., Guilloteau, S., & Ho, P. 2007, in Protostars and Planets V, ed. B. Reipurth, D. Jewitt, & K. Keil (Tucson: Univ. Arizona Press), 495
Edris, K. A., Fuller, G. A., & Cohen, R. J. 2007, A&A, 465, 865
Evans, N. J. 1999, ARA&A, 37, 311
Ferreira, J., Dougados, C., & Cabrit, S. 2006, A&A, 453, 785
Fleming, T. P., & Stone, J. M. 2003, ApJ, 585, 908
Fleming, T. P., Stone, J. M., & Hawley, J. F. 2000, ApJ, 530, 464
Font, A. S., McCarthy, I. G., Johnstone, D., & Ballantyne, D. R. 2004, ApJ, 607, 890
Fromang, S., Terquem, C., & Balbus, S. A. 2002, MNRAS, 329, 18
Fromang, S., Terquem, C., & Nelson, R. P. 2005, MNRAS, 363, 943
Galli, D., Lizano, S., Shu, F. H., & Allen, A. 2006, ApJ, 647, 374
Gammie, C. F. 1996, ApJ, 457, 355
Gammie, C. F., & Johnson, B. M. 2005, in ASP Conf. Ser. 341, Chondrites and the Protoplanetary Disk, ed. A. N. Krot, E. R. D. Scott, & B. Reipurth (San Francisco: ASP), 145
Girart, J. M., Rao, R., & Marrone, D. 2006, Science, 313, 812
Goldreich, P., Lithwick, Y., & Sari, R. 2004, ARA&A, 42, 549
Goldreich, P., & Lynden-Bell, D. 1969, ApJ, 156, 59
Goldreich, P., & Sridhar, S. 1997, ApJ, 485, 680
Goodman, J., & Xu, G. 1994, ApJ, 432, 213
Goodson, A. P., Bohm, K. H., & Winglee, R. M. 1999, ApJ, 524, 142
Gruzinov, A. V., & Diamond, P. H. 1994, Phys. Rev. Lett., 72, 1651
———. 1996, Phys. Plasmas, 3, 1853
Gullbring, E., Hartmann, L., Briceno, C., & Calvet, N. 1998, ApJ, 492, 323
Haisch, K. E., Lada, E. A., & Lada, C. J. 2001, ApJ, 553, L153
Halwachs, J. L., Arenou, F., Mayor, M., Udry, S., & Queloz, D. 2000, A&A, 355, 581
Hartmann, L., Calvet, N., Gullbring, E., & D'Alessio, P. 1998, ApJ, 495, 385
Hartmann, L., & Kenyon, S. J. 1996, ARA&A, 34, 207
Hawley, J. F., & Balbus, S. A. 1991, ApJ, 381, 496
Hayashi, C., Nakazawa, K., & Nakagawa, Y. 1985, in Protostars and Planets II, ed. D. C. Black & M. S. Matthews (Tucson: Univ. Arizona Press), 1100
Herbig, G. H. 1977, ApJ, 217, 693
Herbig, G. H., Petrov, P. P., & Duemmler, R. 2003, ApJ, 595, 384
Hutawarakorn, B., & Cohen, R. J. 2005, MNRAS, 357, 338
Igea, J., & Glassgold, A. E. 1999, ApJ, 518, 848
Jijina, J., Myers, P. C., & Adams, F. C. 1999, ApJS, 125, 161
Jørgensen, J. K., et al. 2007, ApJ, 659, 479
King, A. R., Pringle, J. E., & Livio, M. 2007, MNRAS, 376, 1740
Königl, A., & Pudritz, R. E. 2000, in Protostars and Planets IV, ed. V. Mannings, A. P. Boss, & S. S. Russell (Tucson: Univ. Arizona Press), 759
Krasnopolsky, R., & Gammie, C. F. 2005, ApJ, 635, 1126
Krasnopolsky, R., & Königl, A. 2002, ApJ, 580, 987
Küker, M., Henning, Th., & Rüdiger, G. 2004, Ap&SS, 292, 599
Kwan, J., Fischer, W., Edwards, S., & Hillenbrand, L. 2005, in Protostars and Planets V Abstracts (Houston: LPI), http://www.lpi.usra.edu/meetings/ppv2005/pdf/8076.pdf
Levy, E. H., & Sonett, C. P. 1978, in Protostars and Planets, ed. T. Gehrels (Tucson: Univ. Arizona Press), 516
Lin, D. N. C. 2006, in Planet Formation, ed. H. Klahr & W. Brandner (Cambridge: Cambridge Univ. Press), 256
Lin, D. N. C., & Papaloizou, J. 1996, ARA&A, 34, 703
Lissauer, J. J. 1993, ARA&A, 31, 129
Long, M., Romanova, M. M., & Lovelace, R. V. E. 2005, ApJ, 634, 1214
Lubow, S. H., Papaloizou, J. C. B., & Pringle, J. E. 1994, MNRAS, 267, 235 (LPP94)
Lynden-Bell, D. 1969, Nature, 223, 690
Lynden-Bell, D., & Pringle, J. E. 1974, MNRAS, 168, 603
Marcy, G. W., & Butler, P. R. 2000, PASP, 112, 137
McKeegan, K. 2006, in AGU Meeting Abstracts (Washington: AGU), abstract P52B-03
Mestel, L., & Spitzer, L. 1956, MNRAS, 116, 503
Miller, K. A., & Stone, J. M. 2000, ApJ, 534, 398 (MS00)
Nakano, T., & Nakamura, T. 1978, PASJ, 30, 671
Ogilvie, G. I. 1997, MNRAS, 288, 63
Osorio, M., Lizano, S., & D'Alessio, P. 1999, ApJ, 525, 808
Papaloizou, J., & Lin, D. N. C. 1995, ARA&A, 33, 505
Parker, E. N. 1955, ApJ, 122, 293
———. 1963, Interplanetary Dynamical Processes (New York: Wiley)
———. 1966, ApJ, 145, 811
Pessah, M. E., Chan, C., & Psaltis, D. 2006, MNRAS, submitted (astro-ph/0612404)
Popham, R., Kenyon, S., Hartmann, L., & Narayan, R. 1996, ApJ, 473, 422
Prandtl, L. 1925, Z. Angew. Math. Mech., 5, 136
Pringle, J. 1981, ARA&A, 19, 137
Pudritz, R. E., & Matsumura, S. 2004, Rev. Mex. AA Ser. Conf., 22, 108
Rafikov, R. 2007, ApJ, 662, 642
Reipurth, B., & Bally, J. 2001, ARA&A, 39, 403
Rüdiger, G., & Shalybkov, D. A. 2002, A&A, 393, L81
Sano, T., Miyama, S. M., Umebayashi, T., & Nakano, T. 2000, ApJ, 543, 486 (S00)
Sari, R., & Goldreich, P. 2004, ApJ, 606, L77
Shakura, N. I., & Sunyaev, R. A. 1973, A&A, 24, 337
Shu, F., Najita, J., Ostriker, E., Wilkin, F., Ruden, S., & Lizano, S. 1994, ApJ, 429, 781
Shu, F. H. 1995, Rev. Mex. AA Ser. Conf., 1, 375
Shu, F. H., Adams, F. C., & Lizano, S. 1987, ARA&A, 25, 23
Shu, F. H., Allen, A., Shang, H., Ostriker, E. C., & Li, Z. Y. 1999, in The Origin of Stars and Planetary Systems, ed. C. Lada & N. Kylafis (Dordrecht: Kluwer), 193
Shu, F. H., Galli, D., Lizano, S., & Cai, M. 2006, ApJ, 647, 382
Shu, F. H., & Li, Z.-Y. 1997, ApJ, 475, 251
Shu, F. H., Li, Z.-Y., & Allen, A. 2004, ApJ, 601, 930

Shu, F. H., Shang, H., Glassgold, A. E., & Lee, T. 1997, Science, 277, 1475
Shu, F. H., Shang, H., & Lee, T. 1996, Science, 271, 1545
Shu, F. H., Tremaine, S., Adams, F. C., & Ruden, S. P. 1990, ApJ, 358, 495
Shu, F. H., et al. 2000, in Protostars and Planets IV, ed. V. Mannings, A. P. Boss, & S. S. Russell (Tucson: Univ. Arizona Press), 789
Silver, L. J., & Balbus, S. A. 2006, in SF2A-2006: Proc. Annual Meeting of the French Society of Astronomy and Astrophysics, ed. D. Barret, F. Casoli, G. Lagache, A. Lecavelier, & L. Pagani (Meudon: Obs. Paris), 107
Stacey, F. D. 1976, Annu. Rev. Earth Planet. Sci., 4, 147
Stauber, P., Doty, S. D., van Dishoeck, E. F., Jørgensen, J. K., & Benz, A. O. 2007, A&A, in press
Stone, J. M., Hawley, J. F., Gammie, C. F., & Balbus, S. A. 1996, ApJ, 463, 656 (S96)
Strauss, H. R. 1976, Phys. Fluids, 19, 134
Terquem, C. 2003, MNRAS, 341, 1157
Toomre, A. 1964, ApJ, 139, 1217
van Ballegooijen, A. A. 1989, in Accretion Disks and Magnetic Fields in Astrophysics, ed. G. Belvedere (Dordrecht: Kluwer), 99
Vishniac, E. T., & Diamond, P. H. 1989, ApJ, 347, 435
Vorobyov, E. I., & Basu, S. 2006, ApJ, 650, 956
Wardle, M., & Königl, A. 1993, ApJ, 410, 218
Wardle, M., & Ng, C. 1999, MNRAS, 303, 239
White, R. J., Greene, T. P., Doppmann, G. W., Covey, K. R., & Hillenbrand, L. A. 2007, in Protostars and Planets V, ed. B. Reipurth, D. Jewitt, & K. Keil (Tucson: Univ. Arizona Press), 117
Wünsch, R., Gawryzczak, A., Klahr, H., & Rózyczka, M. 2006, MNRAS, 367, 773
Youdin, A., & Shu, F. H. 2002, ApJ, 580, 494
Young, C. H., & Evans, N. J. 2005, ApJ, 627, 293
Young, C. H., Shirley, Y. L., Evans, N. J., & Rawlings, N. M. C. 2003, ApJS, 145, 111
Zolensky, M. E., et al. 2006, Science, 314, 1735